공학석사학위논문

Dynamic Splitting and Uniaxial Tensile Test Methods to Obtain Dynamic Increase Factor of Concrete in Tension

콘크리트의 인장 동적증가계수 획득을 위한
동적 쪼갬과 일축인장 실험 방법

2022 년 2 월

서울대학교 대학원

건설환경공학부

이 겨 레

Dynamic Splitting and Uniaxial Tensile Test Methods to Obtain Dynamic Increase Factor of Concrete in Tension

콘크리트의 인장 동적증가계수 획득을 위한
동적 쪼갬과 일축인장 실험 방법

지도 교수 조 재 열

이 논문을 공학석사 학위논문으로 제출함
2022 년 2 월

서울대학교 대학원
건설환경공학부
이 겨 레

이겨레의 공학석사 학위논문을 인준함
2022 년 2 월

위 원 장 김 호 경

부위원장 조 재 열

위 원 문 구 학

ABSTRACT

Dynamic Splitting and Uniaxial Tensile Test Methods to Obtain Dynamic Increase Factor of Concrete in Tension

Lee, Kyeore

Department of Civil & Environmental Engineering

The Graduate School

Seoul National University

Loading caused by extreme events that have a much longer return period than the normal design life is characterized as dynamic loading. Dynamic loading imposes a high deformation rate on a structure, and the structural behavior under extreme events is different from that of the static loading condition. Therefore, for the accurate analysis and economical design of structures under extreme events, the dynamic material properties should be investigated in advance.

Concrete, one of the typical construction materials, has rate-dependent properties. In other words, the material properties of concrete vary depending on the strain rate. Important factors are compressive strength and tensile strength, and each strength of concrete becomes greater as the strain rate increases. Dynamic increase factor (DIF) is used to consider a strength

enhancement based on this rate effect, and it is expressed as the ratio of the dynamic material property to the static material property.

In particular, the tensile strength enhancement of concrete expressed by tensile DIF is very important for three reasons. Firstly, in the high strain rate region of 1 to 100 s^{-1}, the tensile strength is increased by about 2 to 6 times compared to the static tensile strength. Since it has a relatively more enhancement ratio than the compressive strength that is increased by about 1 to 2 times in the similar strain rate region, the tensile strength at the high strain rate is an important consideration. Secondly, the dynamic tensile strength controls the tensile failure of structures made of concrete-like materials subjected to impact or blast loading, which means that it influences dominantly on fragmentation, spalling, and scabbing phenomena in the structures. Thirdly, the use of different tensile DIF models results in different failure modes in numerical simulations of an actual structure. For these reasons, it is necessary to investigate the exact tensile DIF to understand the structural behavior subjected to dynamic loading.

Many researchers have proposed tensile DIF of concrete by performing the static and dynamic tensile tests, and various tensile DIF is also presented in several design codes. However, unlike the static tensile test in which a standard test method has been presented, any standard test method for the dynamic tensile test has not been established yet. Different researchers have performed the dynamic tensile tests in different ways, and consequently, proposed tensile DIF is different from each other. Therefore, it is necessary to obtain accurate tensile DIF through a consistent dynamic tensile test.

In this study, through a series of the preliminary tests, test methods for the dynamic splitting and uniaxial tensile tests were proposed, respectively. And by applying the proposed test method, the main test was performed to obtain splitting and direct tensile DIFs of concrete. To develop tensile DIF versus strain rate curves, the static tensile test to obtain the quasi-static value of the strain rate where tensile DIF is taken as 1.0 was also performed. With the reliable data, splitting and direct tensile DIF models through a regression analysis were suggested, respectively. The difference between the suggested splitting and direct tensile DIFs increased as the strain rate increased, and tensile DIF ratio was suggested to investigate the relation between the two tensile DIF models of concrete.

It is expected that proposed dynamic tensile test methods and suggested tensile DIF models of concrete in this study can be applied to the analysis and design of concrete structures under extreme events.

Keywords: splitting tensile test, uniaxial tensile test, splitting tensile strength, direct tensile strength, tensile dynamic increase factor, strain rate, standard test method

Student Number: 2020-23033

TABLE OF CONTENTS

LIST OF TABLES ····· **vii**

LIST OF FIGURES ····· **viii**

NOTATIONS ····· **xi**

1. Introduction ····· **1**

1.1. Research Background ····· 1

1.2. Research Objectives and Scope ····· 9

1.3. Outline ····· 10

2. Theoretical Background ····· **11**

2.1. Splitting tensile test ····· 12

2.1.1. Static splitting tensile test ····· 12

2.1.2. Dynamic splitting tensile test ····· 14

2.1.3. Requirements for the dynamic splitting tensile test method ·· 18

2.1.3.1 Specimen dimension ····· *18*

2.1.3.2 Specimen mounting method ····· *20*

2.2. Uniaxial tensile test ····· 24

2.2.1. Static uniaxial tensile test ····· 24

2.2.2. Dynamic uniaxial tensile test ····· 27

2.2.3. Requirements for dynamic uniaxial tensile test method ····· 31

2.2.3.1 Condition of the notch ····· *31*

2.2.3.2 Amount of the notch ····· *33*

3. Experimental Program ····· 34

3.1. Preliminary splitting tensile test ····· 34

3.1.1. 1st preliminary test ····· 34

3.1.1.1 Test conditions ····· *34*

3.1.1.2 Data post-processing and test results ····· *38*

3.1.1.3 Concluding remarks ····· *43*

3.1.2. 2nd preliminary test ····· 43

3.1.2.1 Test conditions ····· *43*

3.1.2.2 Data post-processing and test results ····· *47*

3.1.2.3 Concluding remarks ····· *52*

3.2. Preliminary uniaxial tensile test ····· 52

3.2.1. 1st preliminary test ····· 52

3.2.1.1 Test conditions ····· *52*

3.2.1.2 Data post-processing and test results ····· *56*

3.2.1.3 Concluding remarks ····· *57*

3.2.2. 2nd preliminary test ····· 57

3.2.2.1 Test conditions ····· *57*

3.2.2.2 Data post-processing and test results ····· *59*

3.2.2.3 Concluding remarks ····· *60*

3.3. Main test ····· 61

3.3.1. Test variables ····· 61
3.3.2. Specimen preparation ····· 63
3.3.3. Data post-processing and test results ····· 64

4. Tensile DIF of Concrete ····· 70
4.1 Suggestion of tensile DIF model of concrete ····· 70
4.2 Relationship between splitting and direct tensile DIFs ····· 75
4.2.1. Comparison between splitting and direct tensile DIFs ····· 75
4.2.2. Derivation of tensile DIF ratio along with the strain rate ····· 76

5. Conclusions ····· 78

Reference ····· 80

국문초록 ····· **85**

LIST OF TABLES

Table 2.1 Characteristics of the static tensile tests of concrete ····· 11
Table 2.2 Characteristics of the dynamic tensile tests of concrete ····· 12
Table 2.3 Previous studies of the dynamic splitting tensile test for concrete-like materials (SHPB diameter and specimen dimension)····· 20
Table 2.4 Previous studies of the dynamic splitting tensile test for concrete-like materials (Specimen mounting method)····· 22
Table 3.1 Test variables of 1st preliminary test (Splitting tensile) ····· 36
Table 3.2 Static tensile test results of 1st preliminary test (Splitting tensile) · 43
Table 3.3 Test variables of 2nd preliminary test (Splitting tensile)····· 45
Table 3.4 Test variables of 1st preliminary test (Uniaxial tensile) ····· 53
Table 3.5 Test variables of 2nd preliminary test (Uniaxial tensile)····· 58
Table 3.6 Test variables of the main test····· 62
Table 3.7 Concrete mix proportion of the main test····· 63
Table 3.8 Static compressive strength test results of the main test ····· 64
Table 3.9 Static tensile test results of the main test ····· 69

LIST OF FIGURES

Figure 1.1 Strain rate in accordance with various events ····· 1
Figure 1.2 Variation of the experimentally obtained compressive DIF with the strain rate (Xu and Wen 2013) ····· 3
Figure 1.3 Variation of the experimentally obtained tensile DIF with the strain rate (Xu and Wen 2013) ····· 3
Figure 1.4 Tensile failure of the structures made of concrete-like materials ··· 4
Figure 1.5 Effect of tensile DIF on cratering and scabbing phenomena ····· 5
Figure 1.6 Various tensile DIFs ····· 7
Figure 2.1 Stress distribution in the specimen of the splitting tensile test ···· 13
Figure 2.2 Designed aligning jig in the static splitting tensile test ····· 14
Figure 2.3 Test setup of the dynamic splitting tensile test using SHPB ····· 15
Figure 2.4 Strain waves and forces on the specimen ends ····· 16
Figure 2.5 High-speed camera setup in the dynamic splitting tensile test ···· 18
Figure 2.6 Schematics of specimen mounting method ····· 22
Figure 2.7 Steel rings and a specimen in the uniaxial tensile test ····· 25
Figure 2.8 Stress distribution in the specimen of the uniaxial tensile test ···· 25
Figure 2.9 Designed linkage system in the static uniaxial tensile test ····· 27
Figure 2.10 Test setup of the dynamic uniaxial tensile test using high-speed hydraulic machine ····· 28
Figure 2.11 The inertial force correction in the dynamic uniaxial tensile test 29
Figure 2.12 Pre-test in the dynamic uniaxial tensile test with only steel rings ····· 30
Figure 2.13 Notched specimen using the diamond blade saw (Li and Ansari 2000) ····· 32
Figure 2.14 Schematics of test setup (Li and Ansari 2000) ····· 32

Figure 3.1 Designation of 1st preliminary test specimen group (Splitting tensile) ····· 36
Figure 3.2 Test specimen of 1st preliminary test (Splitting tensile)····· 36
Figure 3.3 SHPB apparatus of EPTC in SNU ····· 37
Figure 3.4 MTS 815 with the aligning jig in SNU ····· 37
Figure 3.5 Dynamic splitting tensile stress-time relationship with different *R* values; (a) 3%; (b) 36%····· 39
Figure 3.6 Tensile DIF of 1st preliminary test (Splitting tensile) ····· 40
Figure 3.7 *R* values according to the specimen dimension of 1st preliminary test (Splitting tensile); (a) L/D ratio 1.0; (b) L/D ratio 0.5 ····· 41
Figure 3.8 *R* values according to the specimen dimension of 1st preliminary test (Splitting tensile); (a) D75; (b) D50····· 42
Figure 3.9 Designation of 2nd preliminary test specimen group (Splitting tensile) ····· 45
Figure 3.10 Designed FBD D75 steel mold; (a) Drawing detail (b) Actual mold····· 46
Figure 3.11 Test specimen of 2nd preliminary test (Splitting tensile); (a) Flat loading platen (b) FBD ····· 46
Figure 3.12 Tensile DIF of 2nd preliminary test (Splitting tensile) ····· 48
Figure 3.13 *R* values of 2nd preliminary test (Splitting tensile) ····· 49
Figure 3.14 Crack initiation points of 2nd preliminary test (Splitting tensile, impact velocity: 10 m/s, flat loading platen method); (a) Overall failure pattern; (b) Dynamic splitting tensile stress at each image point····· 50
Figure 3.15 Crack initiation points of 2nd preliminary test (Splitting tensile, impact velocity: 10 m/s, FBD method); (a) Overall failure pattern; (b) Dynamic splitting tensile stress at each image point····· 51
Figure 3.16 Designation of 1st preliminary test specimen group (Uniaxial tensile) ····· 53

Figure 3.17 Effective cross-sectional area ratio of 1st preliminary test (Uniaxial tensile) ····· 53
Figure 3.18 Overall epoxy curing process ····· 54
Figure 3.19 Test specimen of 1st preliminary test (Uniaxial tensile) ····· 55
Figure 3.20 MTS 810 with the linkage system in SNU ····· 55
Figure 3.21 Tensile failure behavior of 1st preliminary test (Uniaxial tensile); (a) UN; (b) N-D8; (c) N-D4 ····· 57
Figure 3.22 Designation of 2nd preliminary test specimen group (Uniaxial tensile) ····· 58
Figure 3.23 Effective cross-sectional area ratio of 2nd preliminary test (Uniaxial tensile) ····· 58
Figure 3.24 High-speed hydraulic machine of EPTC in SNU ····· 59
Figure 3.25 Tensile failure behavior of 2nd preliminary test (Uniaxial tensile); (a) D4; (b) D2; ····· 60
Figure 3.26 Designation of the main test specimen group ····· 62
Figure 3.27 Test specimen of the main test; (a) Splitting tensile test; (b) Uniaxial tensile test ····· 64
Figure 3.28 *R* values of the main test ····· 66
Figure 3.29 Data-processing of the main test (Uniaxial tensile); (a) Dynamic direct tensile stress-time relationship; (b) Before and the after of the observed crack occurrence images ····· 67
Figure 3.30 Validation of obtained test data in the main test ····· 68
Figure 3.31 Tensile DIF of the main test ····· 69
Figure 4.1 Tensile DIF of concrete according to the static compressive strength; (a) Splitting tensile DIF; (b) Direct tensile DIF ····· 71
Figure 4.2 Splitting tensile test data and regression equation ····· 73
Figure 4.3 Uniaxial tensile test data and regression equation ····· 74
Figure 4.4 Suggested splitting and direct tensile DIF regression equations ·· 76
Figure 4.5 Tensile DIF ratio between splitting and direct tensile DIFs ····· 77

NOTATIONS

Symbol		Definition and description
A_b	=	The cross-sectional area of bar components
A_s	=	The cross-sectional area of a specimen
DIF	=	Dynamic increase factor
DIF_d	=	Direct tensile DIF
DIF_{ratio}	=	The ratio of splitting tensile DIF to direct tensile DIF
DIF_{sp}	=	Splitting tensile DIF
E_b	=	Young's modulus of bar components
E_s	=	Young's modulus of a specimen
F	=	The internal force of a specimen
F_{lw}	=	Force measured by a load washer
F_m	=	The material parameter in the formula of Xu and Wen (2013)
P	=	Applied loading to a specimen
P_1	=	The force of interface between specimen and incident bar
P_2	=	The force of interface between specimen and transmitted bar
R	=	The parameter of dynamic stress equilibrium
S	=	The material parameter in the formula of Xu and Wen (2013)
T	=	Time to reach the maximum value of stress

W_x	=	The material parameter in the formula of Xu and Wen (2013)
W_y	=	The material parameter in the formula of Xu and Wen (2013)
a_2	=	Acceleration of a bottom grip
d_s	=	Diameter of a specimen
$f_c^{'}$	=	Compressive strength of concrete
$f_{co}^{'}$	=	Reference compressive strength of concrete in Malvar and Crawford (1998)
$f_{d,static}$	=	Static direct tensile strength of concrete
$f_{sp,static}$	=	Static splitting tensile strength of concrete
f_{dd}	=	Dynamic direct tensile strength of concrete
f_{spd}	=	Dynamic splitting tensile strength of concrete
$f_{spd,back}$	=	Dynamic splitting tensile strength of back stress
$f_{spd,front}$	=	Dynamic splitting tensile strength of front stress
k_1	=	The first parameter in the suggested tensile DIF
k_2	=	The second parameter in the suggested tensile DIF
l_s	=	Length of a specimen
m_2	=	The effective mass of a bottom grip
β	=	The material parameter in the formula of Malvar and Crawford (1998)
δ	=	The material parameter in the formula of Malvar and Crawford (1998)
ε	=	Strain
ε_i	=	Incident strain wave

ε_r	=	Reflected strain wave
ε_t	=	Transmitted strain wave
$\dot{\varepsilon}$	=	Strain rate
$\dot{\varepsilon}_0$	=	Reference strain rate in Xu and Wen (2013)
$\dot{\varepsilon}_s$	=	Reference strain rate in Malvar and Crawford (1998) and fib MC2010
$\dot{\varepsilon}_{s,static}$	=	The quasi-static strain rate of a specimen under static tensile test
γ	=	The effective cross-sectional area ratio of a specimen
σ	=	Stress
$\sigma_{d,dynamic}$	=	Dynamic direct tensile stress of a specimen
$\sigma_{d,static}$	=	Static direct tensile stress of a specimen
$\sigma_{sp,1}$	=	Splitting tensile stress of interface between specimen and incident bar
$\sigma_{sp,2}$	=	Splitting tensile stress of interface between specimen and transmitted bar
$\sigma_{sp,FBD}$	=	Splitting tensile stress of a specimen in FBD method
$\sigma_{sp,dynamic}$	=	Dynamic splitting tensile stress of a specimen
$\sigma_{sp,static}$	=	Static splitting tensile stress of a specimen
σ_x	=	Stress in the *x*-axis direction
σ_y	=	Stress in the *y*-axis direction

1. Introduction

1.1. Research Background

Extreme events, which are natural disasters such as typhoons and earthquakes, or human disasters such as impacts and blasts, have been occurring frequently in recent years. As the probability that the structures suffer from these extreme events during their design life increases, many related studies have been conducted. Loading caused by extreme events is characterized as dynamic loading. This dynamic loading causes a high deformation rate on the structure and makes the material behave differently from the static loading condition as shown in Figure 1.1. Therefore, it is necessary to investigate the dynamic material properties for the accurate analysis and economical design of the structures under extreme events.

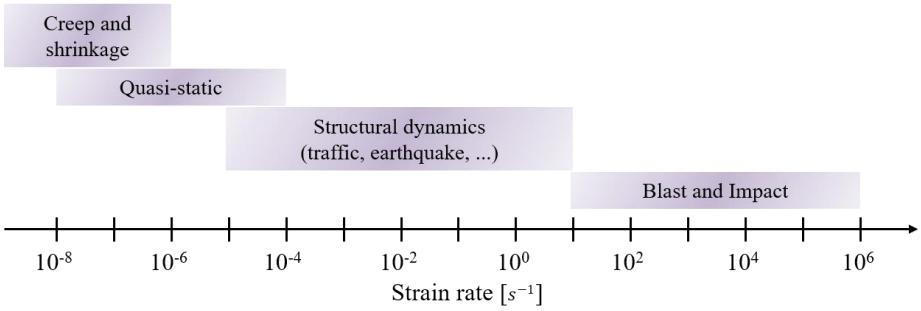

Figure 1.1 Strain rate in accordance with various events

Concrete is an essential construction material and has rate-dependent properties, that is, material properties of concrete vary along with the strain rate. Especially, the compressive strength and tensile strength of concrete

become greater as the strain rate increases. This rate dependence of concrete behavior is called as rate effect and is assumed to be caused by two different physical mechanisms (Cusatis 2011).

1. The fracture process on the rate of crack opening

2. The viscoelastic deformation of the unfractured cement paste

To consider the strength enhancement based on this rate effect, the dynamic increase factor (DIF) defined as the ratio of the dynamic material property to the static material property as shown in Eq. 1.1 is used. Usually, DIF is used in a constitutive equation in the structural analysis, and in the structural design, DIF is used as a factor multiplied by a static strength. In this study, DIF of concrete tensile strength as shown in Eq. 1.2 was only covered.

$$DIF = \frac{(\text{Dynamic material property})}{(\text{Static material property})} \tag{1.1}$$

$$DIF = \frac{(\text{Dynamic tensile strength})}{(\text{Static tensile strength})} \tag{1.2}$$

Meanwhile, the tensile strength enhancement of concrete expressed as tensile DIF is important for three reasons. First of all, the tensile strength increases about 2 to 6 times than the static tensile strength (Malvar and Crawford 1998) in the strain rate of 1 to 100 s^{-1} as shown in Figure 1.2. On the other hand, as shown in Figure 1.3 representing compressive DIF, the compressive strength increases about 1 to 2 times than the static compressive strength in the same strain rate (1-100 s^{-1}). Therefore, the tensile strength,

which is usually neglected due to its small value in the static state, is a major consideration at high strain rate.

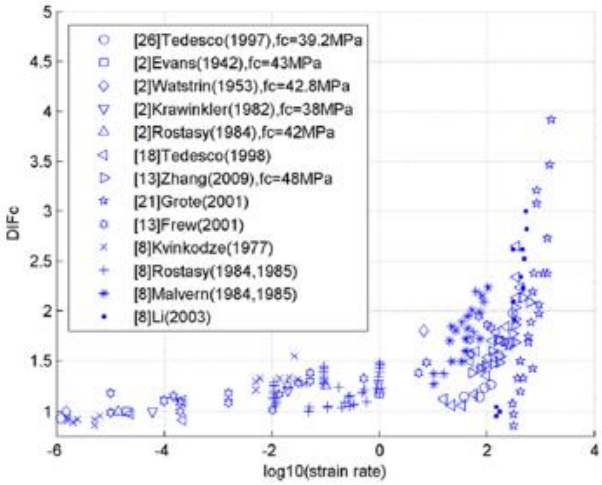

Figure 1.2 Variation of the experimentally obtained compressive DIF with the strain rate (Xu and Wen 2013)

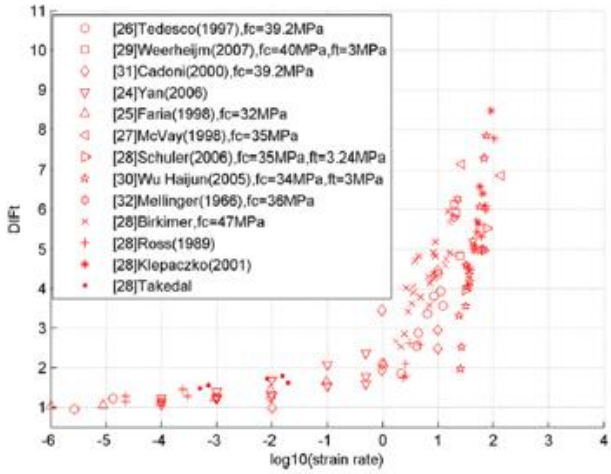

Figure 1.3 Variation of the experimentally obtained tensile DIF with the strain rate (Xu and Wen 2013)

Secondly, the dynamic tensile strength controls the tensile failure of the structures made of concrete-like materials subjected to impact or blast loading (Lu and Li 2011). That is, the tensile strength has a dominant influence not only on fragmentation but also spalling and scabbing phenomena which are local failure modes of the structures as shown in Figure 1.4.

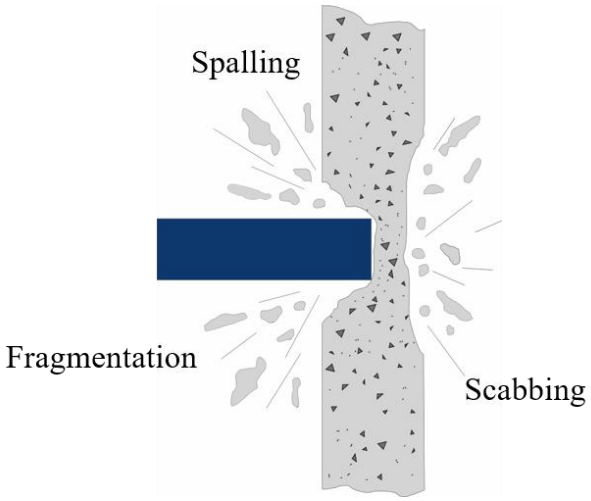

Figure 1.4 Tensile failure of the structures made of concrete-like materials

Thirdly, when conducting an analytical investigation into the tensile strength influencing the failure mode of an actual structure, the numerical simulation results of the failure mode vary depending on tensile DIF model used (Kong et al. 2017). Kong et al. (2017) numerically simulated a penetration of concrete slab subjected to projectile impact and conducted parametric studies for tensile DIF. The influence of tensile DIF on cratering and scabbing phenomena was presented as shown in Figure 1.5.

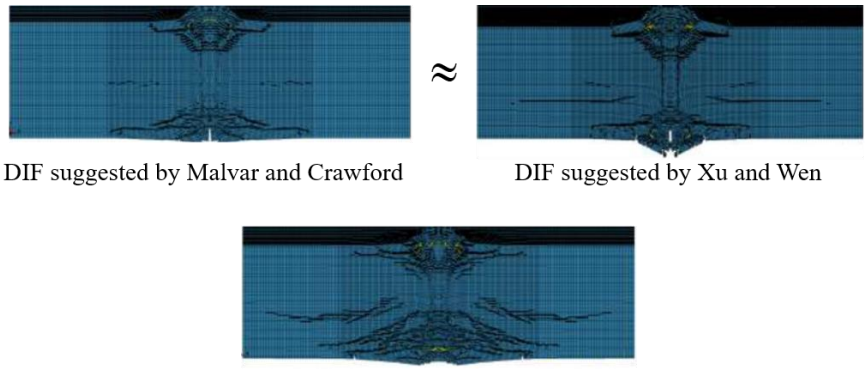

Figure 1.5 Effect of tensile DIF on cratering and scabbing phenomena

It was concluded that when using tensile DIF models of Malvar and Crawford (1998) and Xu and Wen (2013), which are close to each other, the cratering and scabbing phenomena from each tensile DIF were very similar. On the other hand, when the CEB MC 1990 model (1990) that underestimates tensile DIF was used, the scabbing phenomenon was not reproduced well. Hence, an investigation of accurate tensile DIF is needed to understand the structural behavior subjected to dynamic loading.

To obtain tensile DIF of concrete, the static and dynamic tensile tests of concrete should be carried out. Various tensile DIF has been proposed by many researchers, and there is representative tensile DIF by Malvar and Crawford (1998), Xu and Wen (2013), and Liu et al. (2020). Each proposed tensile DIF is shown as Eq. 1.3 through Eq. 1.5.

$$DIF = \begin{cases} \left(\dfrac{\dot{\varepsilon}}{\dot{\varepsilon}_s}\right)^{\delta} & \text{for } 10^{-6}s^{-1} \le \dot{\varepsilon} \le 1s^{-1} \\ \beta\left(\dfrac{\dot{\varepsilon}}{\dot{\varepsilon}_s}\right)^{1/3} & \text{for } 1s^{-1} \le \dot{\varepsilon} \le 160\,s^{-1} \end{cases}$$

$$\text{where, } \log\beta = 6\delta - 2,\ \delta = 1/\left(1 + 8f_c^{'} / f_{co}^{'}\right), \tag{1.3}$$

$$f_{co}^{'} = 10\,\text{MPa},\ \dot{\varepsilon}_s = 1.0\times10^{-6}s^{-1}$$

$$DIF = \left\{\left[\tanh\left(\left(\log\left(\dot{\varepsilon}/\dot{\varepsilon}_0\right) - W_x\right)S\right)\right]\left[\frac{F_m}{W_y} - 1\right] + 1\right\}W_y \tag{1.4}$$

$$\text{where, } \dot{\varepsilon}_0 = 1.0\,s^{-1},\ F_m = 10\ ,\ W_x = 1.6,\ S = 0.8,\ W_y = 5.5$$

$$DIF = 1 + \left(\frac{\dot{\varepsilon}}{5}\right)^{0.876} \tag{1.5}$$

Furthermore, various tensile DIF is also presented in several design codes: fib MC 2010 (Eq. 1.6), ACI 370R-14 (Eq. 1.7), and UFC 3-340-02 (provided by graphs). Figure 1.6 shows tensile DIF of concrete along with the strain rate on a log scale.

$$DIF = \begin{cases} \left(\dfrac{\dot{\varepsilon}}{\dot{\varepsilon}_s}\right)^{0.018} & \text{for } 10^{-6}s^{-1} \le \dot{\varepsilon} \le 10\,s^{-1} \\ 0.0062\left(\dfrac{\dot{\varepsilon}}{\dot{\varepsilon}_s}\right)^{1/3} & \text{for } 10\,s^{-1} \le \dot{\varepsilon} \le 300\,s^{-1} \end{cases} \tag{1.6}$$

$$\text{where, } \dot{\varepsilon}_s = 1.0\times10^{-6}s^{-1}$$

$$DIF = \begin{cases} 0.1424\log_{10}\dot{\varepsilon} + 1.833 \ge 1.0 & \text{for } \dot{\varepsilon} < 2.32\,s^{-1} \\ 2.92\log_{10}\dot{\varepsilon} + 0.814 \le 6.0 & \text{for } \dot{\varepsilon} > 2.32\,s^{-1} \end{cases} \tag{1.7}$$

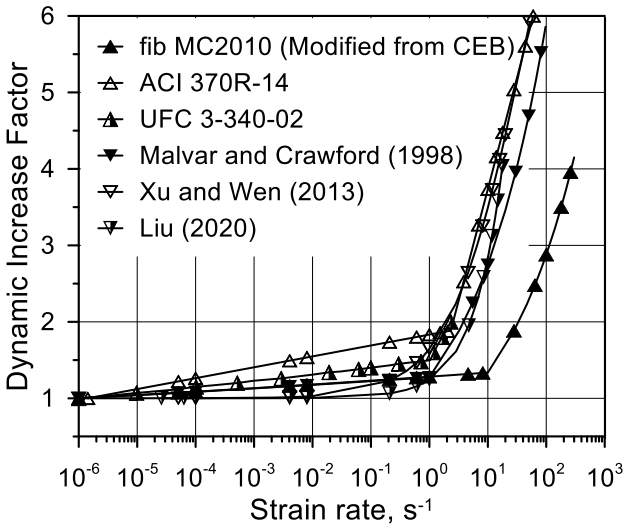

Figure 1.6 Various tensile DIFs

As shown in Figure 1.6, tensile DIF is different from each other because different researchers have performed the dynamic tensile tests in different ways. Unlike the static tensile test in which a standard test method is presented, any dynamic tensile test has not been established with a standard test method due to the scarcity of test apparatus or the absence of guidelines for test techniques. This makes it impossible to build a database on account of a lack of consistency and reliability of test data. Therefore, it is important to establish a standard test method so that a consistent dynamic tensile test can be carried out, and through the established test method, it is necessary to evaluate an accurate tensile DIF.

In this study, splitting and uniaxial tensile tests, which can be carried out on the same principle in both the static and dynamic tests, were investigated. Through a series of the preliminary tests, test methods were proposed for dynamic splitting tensile test using SHPB and dynamic uniaxial tensile test

using high-speed hydraulic machine, respectively. After that, by applying the proposed test method, the main test of splitting tensile and uniaxial tensile tests was carried out to obtain splitting and direct tensile DIF of concrete. Static splitting and uniaxial tensile tests were also performed to obtain each static tensile strength. Then, splitting and direct tensile DIF models were suggested by regression analysis Lastly, discussions on the relationship between the suggested splitting and direct tensile DIFs were conducted.

1.2. Research Objectives and Scope

There are three main objectives in this study. One of the main objectives of this study is a proposal of the test method for the dynamic tensile test. Another main objective is an experimental investigation of tensile DIF of concrete through the proposed test method. The other main objective is the suggestion for tensile DIF model of concrete. The suggested DIF model is divided into splitting and direct tensile DIFs according to the type of tensile strength. With each tensile DIF suggested, the relationship between splitting and direct tensile DIFs was investigated.

For these objectives, this study is divided into three main parts. The first main part is a proposal of the dynamic tensile test method through a series of the preliminary tests. The first main part is divided into two minor parts: the preliminary splitting tensile test and preliminary uniaxial tensile test. Another main part is performing the main test to obtain tensile DIF of concrete. This main part is divided into three minor parts, and each minor part includes test variables, specimen preparation, data post-processing and test results. The other main part is a suggestion for tensile DIF model of concrete. The last main part consists of two minor parts: a nonlinear regression analysis to suggest tensile DIF model and the derivation for tensile DIF ratio of splitting and direct tensile DIFs.

1.3. Outline

Chapter 1 indicates the introduction such as the research background, objectives, scope, and outline of this study.

Chapter 2 presents basic concepts of the static splitting and uniaxial tensile tests of concrete. Then, the description of the requirements for the dynamic splitting and uniaxial tensile test methods based on each static test and previous studies is continued in each section.

Chapter 3 includes the performance of splitting and uniaxial tensile tests. It is divided into the preliminary tests and the main test. In the case of the preliminary tests, test conditions, data-post processing and test results are included. Through the test results, the dynamic splitting and uniaxial tensile test methods were proposed. And in the main test conducted by the proposed test method, both static and dynamic splitting and uniaxial tensile tests performed are described. It includes test variables, specimen preparation, data post-processing and test results. In addition, through validation of test data, obtained tensile DIF of concrete is presented in this chapter.

Chapter 4, by conducting nonlinear regression analysis, splitting and direct tensile DIF models are suggested. Finally, tensile DIF ratio along with the strain rate between splitting and direct tensile DIFs is presented.

Finally, the conclusions of this study are summarized in chapter 5.

2. Theoretical Background

Tensile tests of concrete are divided into direct and indirect tensile tests according to the method of applying tensile stress. In the static tensile test, there is a uniaxial tensile test as a method of applying tensile stress directly, and splitting and flexural tensile tests are regarded as the methods of applying tensile stress indirectly. Each tensile test is presented in American Society for Testing and Materials (ASTM) and Korean Standards (KS) as a standard test method. The characteristics of the static tensile tests of concrete are presented in Table 2.1.

Table 2.1 Characteristics of the static tensile tests of concrete

How to apply tensile stress	Test type	Strength type	Test apparatus
Directly	Uniaxial tensile test	Direct tensile strength	Universal Testing Machine (UTM)
Indirectly	Splitting tensile test	Splitting tensile strength	
	Flexural tensile test	Flexural tensile strength	

There are also three typical dynamic tensile tests: uniaxial tensile test, spalling test, and splitting tensile test. However, as described previously, any standard test method for the dynamic tensile test has not been established yet. The characteristics of the dynamic tensile tests of concrete are presented in Table 2.2.

Table 2.2 Characteristics of the dynamic tensile tests of concrete

How to apply tensile stress	Test type	Strength type	Test apparatus
Directly	Uniaxial tensile test	Direct tensile strength	High-speed hydraulic machine
	Spalling test		Split Hopkinson Pressure Bar (SHPB)
Indirectly	Splitting tensile test	Splitting tensile strength	

In this study, a series of the preliminary tests were carried out to propose the dynamic splitting and uniaxial tensile test methods. Then, with the proposed test methods, the main test was performed. Therefore, basic concepts of the static splitting and uniaxial tensile tests were briefly described, respectively. Then, based on the static test and previous studies of each tensile test, explanations of the requirements for the dynamic splitting and uniaxial tensile test methods are continued in each section.

2.1. Splitting tensile test

2.1.1. Static splitting tensile test

Splitting tensile test, called Brazilian disk test, was developed to indirectly determine the tensile strength of brittle materials using cylindrical specimens. Splitting tensile test has been the most widely performed because the test method is relatively simple rather than other tensile tests. ASTM C496/C496M and KS F 2423 present a standard test method for the static splitting tensile test of concrete.

In general, the static splitting tensile test is carried out with the same test apparatus as the static compressive strength test. The specimen is positioned such that its longitudinal axis lies horizontally between the loading plates. The stress state of the splitting tensile test has an analytical solution if a plane-strain state is assumed and a concentrated line loading is applied (Lu and Li 2011). The stress distribution in the specimen of the splitting tensile test is shown in Figure 2.1.

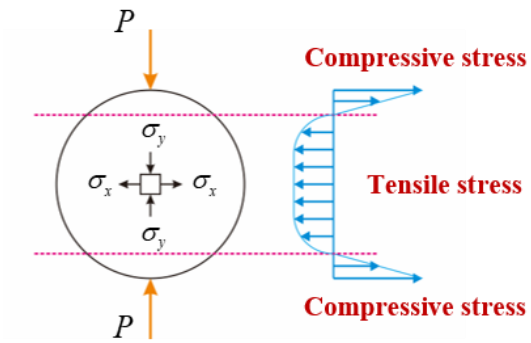

Figure 2.1 Stress distribution in the specimen of the splitting tensile test

Splitting tensile stress is generated at direction vertical to the loading diameter causing the tensile failure of the specimen, and a magnitude of the static splitting tensile stress can be obtained by Eq. 2.1 presented in ASTM C496/C496M according to the elasticity theory.

$$\sigma_{sp,static} = \frac{2P}{\pi d_s l_s} \tag{2.1}$$

Most previous studies recommended the quasi-static strain rate of 10^{-6} s^{-1} in the static splitting tensile tests. An arbitrary loading rate can be determined

by targeting the quasi-static strain rate with the assumption of linear behavior, then the static splitting tensile strength of the specimen can be obtained.

In addition, one of the important things in performing the static splitting tensile test is that the alignment of the specimen to which the loading is applied is maintained. This can be achieved by using a designed aligning jig as shown in Figure 2.2.

Figure 2.2 Designed aligning jig in the static splitting tensile test

By using the aligning jig, the center of the specimen may be located right beneath the loading plate, and the loading can be evenly distributed in the longitudinal direction of the specimen. After correctly mounting the specimen on the aligning jig, the loading is applied at the determined loading rate to induce the tensile failure.

2.1.2. Dynamic splitting tensile test

Dynamic splitting tensile test is also widely performed to obtain the dynamic tensile strength of concrete due to its simplicity compared to other

dynamic tensile tests. Split Hopkinson Pressure Bar (SHPB) has been used as test apparatus same as the dynamic compressive strength test. SHPB was developed by H. Kolsky and usually consists of three main parts: loading device (air gun, striker, and pulse shaper), bar components (incident bar, transmitted bar, and momentum trapping bar), and measurement system (strain gauges on the bar components surfaces). The specimen in the dynamic test is also held diametrically between the incident bar and the transmitted bar. Test setup of the dynamic splitting tensile test using SHPB is shown in Figure 2.3.

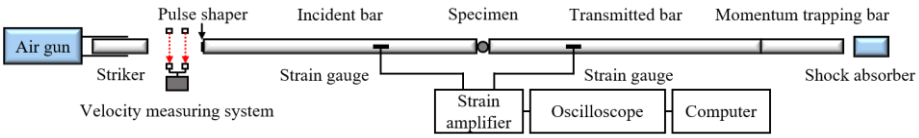

Figure 2.3 Test setup of the dynamic splitting tensile test using SHPB

In order to load the specimen, the incident bar is impacted with the striker fired from the air gun, which creates an incident wave propagating through the incident bar. When the incident wave arrives on the interface between the specimen and the incident bar, part of the incident wave is reflected into the incident bar as a reflected wave; and the other part of the wave propagates the specimen and then is transmitted into the transmitted bar as a transmitted wave. All those strain waves are measured by strain gauges attached to each bar.

The principle of SHPB is based on one-dimensional stress wave theory and it means that the bar components remain linear elastic. Assuming that the

strain waves propagate through both incident and transmitted bars without any dispersion, dynamic splitting tensile stress can be obtained as follows (Chen and Song 2010). Measured strain waves are shifted to the time when the incident wave arrives on the interface between the incident bar and the specimen, and the strain waves are converted to forces at the front and back end surfaces of the specimen as shown in Eq. 2.2 and 2.3. Strain waves and forces on the specimen ends are shown in Figure 2.4.

$$P_1 = E_b A_b \left(\varepsilon_i + \varepsilon_r \right) \tag{2.2}$$

$$P_2 = E_b A_b \varepsilon_t \tag{2.3}$$

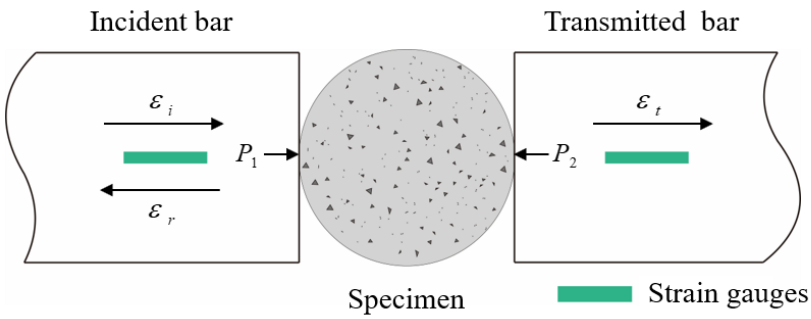

Figure 2.4 Strain waves and forces on the specimen ends

Then, stress at the front and back end surfaces of the specimen can be obtained using the same equation as the static splitting tensile test as in Eq. 2.4 and 2.5. Considering the stress difference between the front and back end surfaces of the specimen, the dynamic splitting tensile stress can be expressed by Eq. 2.6 as an average value.

$$\sigma_{sp,1} = \frac{2P_1}{\pi d_s l_s} \tag{2.4}$$

$$\sigma_{sp,2} = \frac{2P_2}{\pi d_s l_s} \tag{2.5}$$

$$\sigma_{sp,dynamic} = \frac{\sigma_{sp,1} + \sigma_{sp,2}}{2} \tag{2.6}$$

Meanwhile, the strain rate of the specimen is not constant in the dynamic splitting tensile test using SHPB in the loading period (Liu et al. 2020). Therefore, the average strain rate of the specimen can be adopted (Tedesco and Ross 1993). With the assumption that Young's modulus of concrete has no significant dependence on the strain rate (Schuler et al. 2006), the average strain rate of the specimen can be obtained by Eq. 2.7.

$$\dot{\varepsilon} = \frac{f_{spd}}{E_s T} \tag{2.7}$$

Furthermore, the dynamic splitting tensile test may be considered as a valid test if the following conditions are satisfied (Siregar et al. 2007).

1. The stress distribution shows the same behavior as in the static test
2. The indirect tensile failure occurs after the stress distribution is developed
3. The compressive failure that might occur near the impact contact surface should not precede the tensile failure

From the first assumption, it is assumed that the stress distribution in the dynamic splitting tensile test is the same as the static test. As a means of verifying that assumption, it is important to confirm that the crack initiation occurs near the center of the specimen. An effective way to measure the crack initiation point of the specimen is to use a high-speed camera. The researcher can observe the overall failure pattern of the specimen as well as the crack initiation point through the high-speed camera. In this study, a high-speed camera was used as shown in Figure 2.5 to observe the crack initiation point.

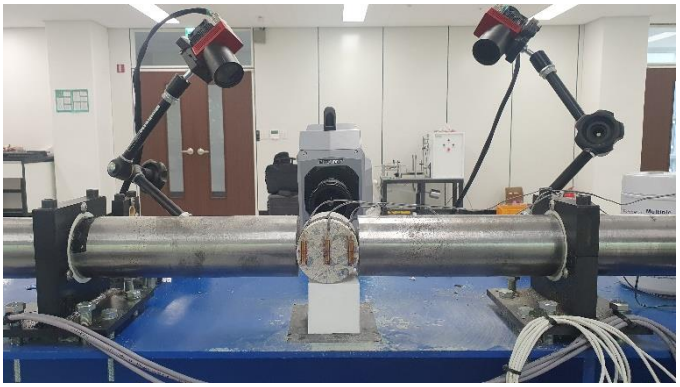

Figure 2.5 High-speed camera setup in the dynamic splitting tensile test

2.1.3. Requirements for the dynamic splitting tensile test method

2.1.3.1 Specimen dimension

In the dynamic splitting tensile test, it is difficult to use a large diameter SHPB apparatus. There are five main reasons for the difficulties as follows (Chen and Song 2010).

1. To satisfy the assumption of one-dimensional stress wave theory, the length of the incident and transmitted bars should be sufficiently long compared to the diameter

2. Stress wave dispersion due to radial inertia of the bars becomes more severe

3. Strain rate is limited due to relatively large specimen size

4. It is difficult to satisfy the stress equilibrium of the specimen

5. Effect of inertia for the specimen becomes more significant

Consequently, dynamic splitting tensile test has been performed using the specimen smaller than the standard cylindrical specimens of the static test. Table 2.3 presents SHPB diameter and the specimen dimension of previous studies conducting the dynamic splitting tensile test for concrete-like materials.

As shown in Table 2.3, the researchers have performed the dynamic splitting tensile test using SHPB with different specimen dimensions. Specimen dimension is expressed in terms of the diameter and the length of the specimen. Experimental strain rate varies according to the specimen dimension, and in addition, specimen dimension affects the dynamic stress equilibrium of the specimen. Therefore, to propose a test method for the dynamic splitting tensile test using SHPB, it is necessary to confirm and determine the appropriate specimen dimension.

Table 2.3 Previous studies of the dynamic splitting tensile test for concrete-like materials (SHPB diameter and specimen dimension)

Reference	Specimen material	SHPB diameter, mm	Specimen dimension, mm
Ross et al. 1989	Concrete Mortar	51	D51×L51 D21×L-
Tedesco et al. 1993	Concrete	50.8	D50.8×L50.8
Lambert and Ross 2000	Concrete	76	D76×L38
Gomez et al. 2001	Concrete Granite	50.8	D50.8×L21.8
Wang et al. 2009	Rock (Marble)	100	D65×L26 D75×L30 D85×L34 D85×L30 D65×L30
Chen et al. 2014	Mortar	74	D74×L30
Yang et al. 2015	Mortar	74	D70×L55
Chen et al. 2017	Concrete	74	D74×L37
Jin et al. 2017	Concrete Mortar	74	D70×L55 D70×L30
Chen et al. 2018	Concrete	74	D70×L50 D70×L30
Liu et al. 2020	Concrete Mortar	50	D63×L35

2.1.3.2 Specimen mounting method

As mentioned before, for satisfying the assumptions of the dynamic splitting tensile test, one of the most important things in the dynamic splitting tensile test is to maintain an ideal contact state between the bar and the specimen. Since the significant compressive stress concentration can cause

premature failure of the specimen at the contact surface, the specimen mounting method is a key factor in the dynamic splitting tensile test. To solve the stress concentration problem, many researchers have proposed several specimen mounting methods: flat loading platen, load-bearing strips, arc loading (including anvils), and Flattened Brazilian Disc (FBD) methods. The characteristics of each specimen mounting method are briefly described as follows.

1. Flat loading platen: Simply mounting a specimen without additional special devices

2. Load-bearing strips: Inserting a flat plank such as plywood between the bar and a specimen

3. Arc loading: Inserting a loading plate having a curvature. At this moment, the radius of curvature of the loading plate should be the same as or greater than the radius of a specimen, and the greater case is called anvil loading

4. Flattened Brazilian Disc (FBD): Mounting a specimen with a flat contact surface

The schematics of each method are shown in Figure 2.6. And, Table 2.4 presents the specimen mounting methods of previous studies conducting the dynamic splitting tensile test for concrete-like materials.

However, as shown in Table 2.4, different specimen mounting methods have been used to prevent premature compressive failure of the specimen due

to the stress concentration. Hence, to propose a test method for the dynamic splitting tensile test using SHPB, the determination of an appropriate specimen mounting method is required.

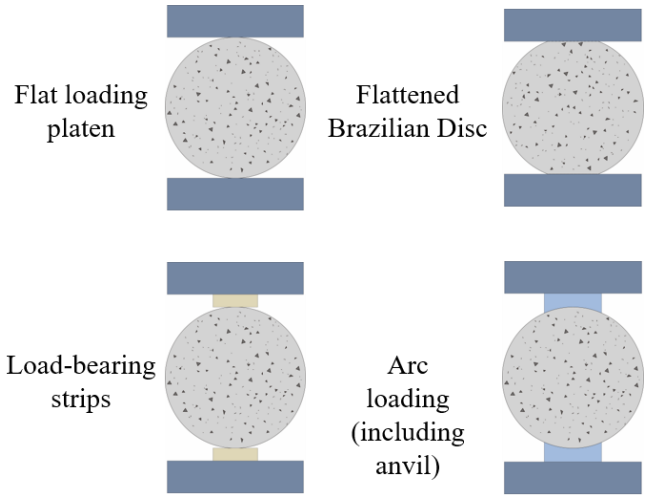

Figure 2.6 Schematics of specimen mounting method

Table 2.4 Previous studies of the dynamic splitting tensile test for concrete-like materials (Specimen mounting method)

Reference	Specimen material	Specimen mounting method	Strain rate, s^{-1}
Ross et al. 1989	Concrete Mortar	Flat loading platen	1-10
Tedesco et al. 1993	Concrete	Load-bearing strips	1-8
Lambert and Ross 2000	Concrete	Load-bearing strips	1-8
Gomez et al. 2001	Concrete Granite	Load-bearing strips	-
Wang et al. 2009	Rock (Marble)	Flattened Brazilian Disc (FBD)	20-30
Chen et al. 2014	Mortar	Flattened Brazilian Disc (FBD)	5-80

Yang et al. 2015	Mortar	Arc loading (anvil)	1-6
Chen et al. 2017	Concrete	Arc loading	-
Jin et al. 2017	Concrete Mortar	Flat loading platen Arc loading (anvil)	20-160
Chen et al. 2018	Concrete	Flat loading platen	20-120
Liu et al. 2020	Concrete Mortar	Flat loading platen	9-20

2.2. Uniaxial tensile test

2.2.1. Static uniaxial tensile test

Uniaxial tensile test has been carried out to obtain the direct tensile strength of concrete. However, there are considerable difficulties in conducting uniaxial tensile tests both in the static and dynamic tests as follows.

1. Design of test setup to assure the concentricity of loading

2. Alignment of a specimen to avoid the eccentricity for proper tensile failure

Because of the above difficulties in the implementation of the test, the uniaxial tensile test has rarely been selected for obtaining the tensile strength. Theoretically, the uniaxial tensile test yields the tensile strength closer to the true strength under pure uniaxial tension. Researchers have developed several variations of the uniaxial tensile tests. Using friction grips to fix the ends of the specimen and applying the tensile loading through some steel studs embedded in concrete have been used. However, these test methods have several problems caused by secondary stress at the ends of the specimen. The major problems include uneven stress distribution, localized failure at the ends, and a significant reduction in the measured tensile strength (Zheng et al. 2001). Therefore, to apply tensile loading without inducing secondary stress, gluing steel rings to the ends of the cylindrical specimen can be used as shown in Figure 2.7.

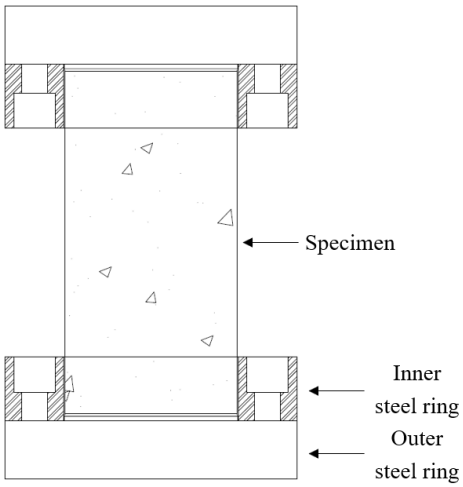

Figure 2.7 Steel rings and a specimen in the uniaxial tensile test

There are two pieces of steel rings. An inner steel ring is glued to the side of the specimen and an outer steel ring is glued to the end of the specimen. The inner and outer steel rings are connected by several bolts, and by pulling the steel rings, the pure tensile loading can be transmitted to the specimen, and cause direct tensile stress as shown in Figure 2.8.

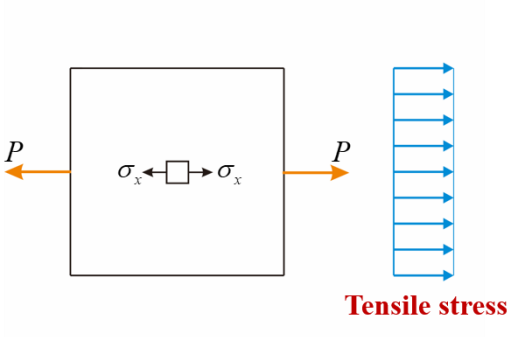

Figure 2.8 Stress distribution in the specimen of the uniaxial tensile test

Direct tensile stress is generated in the direction in which the tensile loading is applied causing the tensile failure of the specimen, and a magnitude of direct tensile stress can be calculated by dividing the tensile loading by the cross-sectional area of the specimen as shown in Eq. 2.8.

$$\sigma_{d,static} = \frac{P}{A_s} \tag{2.8}$$

Static uniaxial tensile test should also target the quasi-static strain rate of 10^{-6} s^{-1} same as the static splitting tensile test. Static direct tensile strength can be obtained at the quasi-static strain rate with an arbitrary loading rate determined assuming linear behavior.

Furthermore, unlike the static splitting tensile test, there is no standard test method for the static uniaxial tensile test of concrete. For the static uniaxial tensile test of concrete, a standard test method of cylindrical rock core specimen presented in ASTM D2936 can be referred to. In order to effectively reduce bending or torsional stresses to the specimen, a linkage system composed of roller chains can be used as presented in ASTM D2936. Schematics of the designed linkage system are shown in Figure 2.9.

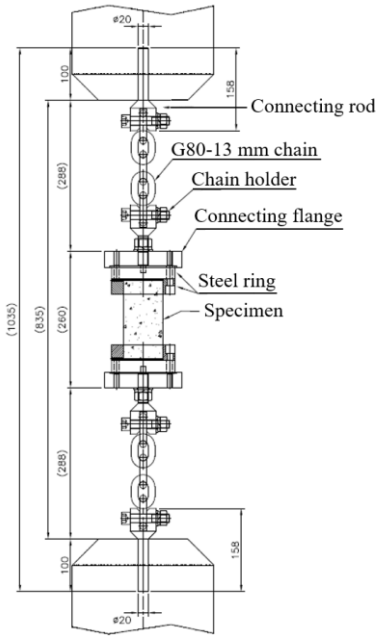

Figure 2.9 Designed linkage system in the static uniaxial tensile test

The linkage system is composed of roller chains, chain holders, and connecting flanges. The roller chains are connected to the chain holder. One end is combined with the connecting flange and the other end is combined with the connecting rod. The connecting flange is fastened with the steel ring and bolts, then the tensile loading is applied directly to the specimen by pulling the connecting rod. Static uniaxial tensile test is performed at the determined loading rate, and the test is terminated when the tensile failure occurs.

2.2.2. Dynamic uniaxial tensile test

Meanwhile, as in the static uniaxial tensile test, the tensile loading can be applied directly by pulling the specimen in the dynamic uniaxial tensile test.

High-speed hydraulic machine can be used to perform the dynamic uniaxial tensile test of concrete. High-speed hydraulic machine consists of a ram, a bottom grip, and a transducer assembly (load washer and accelerometer). Steel rings are connected to the test machine with several bolts. Test setup of the dynamic uniaxial tensile test using the high-speed hydraulic machine is shown in Figure 2.10.

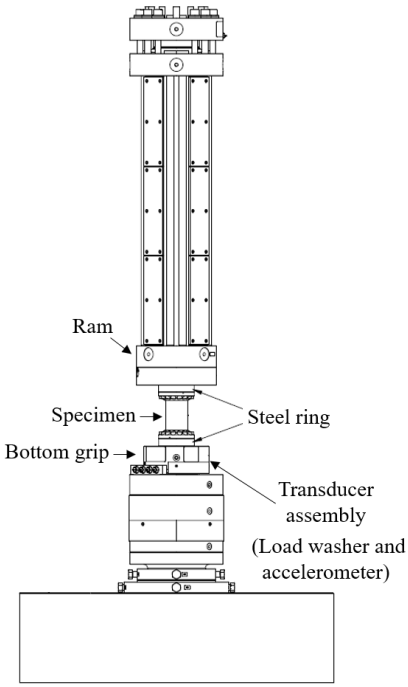

Figure 2.10 Test setup of the dynamic uniaxial tensile test using high-speed hydraulic machine

Principle of the dynamic uniaxial tensile test using high-speed hydraulic machine is same as the static test. The ram moves upward fast with the arbitrary pull-out velocity and pulls the specimen. Pure tensile loading is applied to the specimen and the tensile failure occurs. Meanwhile, in the

dynamic test, the loading applied to the specimen needs the inertial force correction as shown in Figure 2.11. The loading is measured with the load washer in the transducer assembly, but the load washer does not measure the inertial force of the mass of the bottom grip. Hence, the inertial force should be added to the load washer force to evaluate the internal force of the specimen accurately.

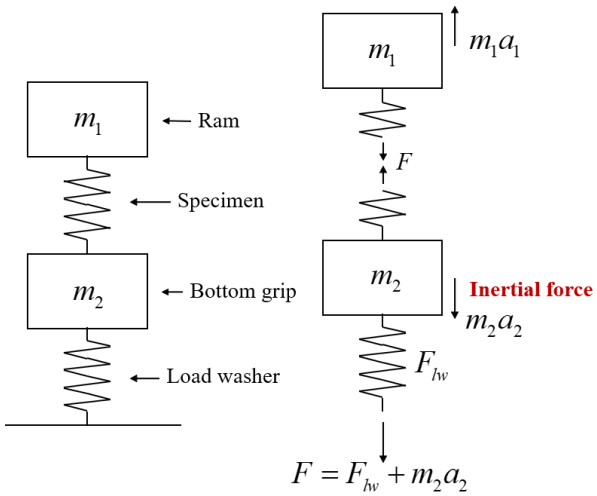

Figure 2.11 The inertial force correction in the dynamic uniaxial tensile test

At this moment, the effective mass of the bottom grip should be determined to calculate the inertial force. The effective mass of the bottom grip can be expressed as Eq. 2.9 in which the resultant force of the load washer force and the inertial force becomes zero: the acceleration of the bottom grip is measured by the load accelerometer in the transducer assembly. And for this purpose, a pre-test should be performed by connecting only the steel rings to the test machine without a specimen as shown in Figure 2.12.

$$m_2 = -\frac{F_{lw}}{a_2} \tag{2.9}$$

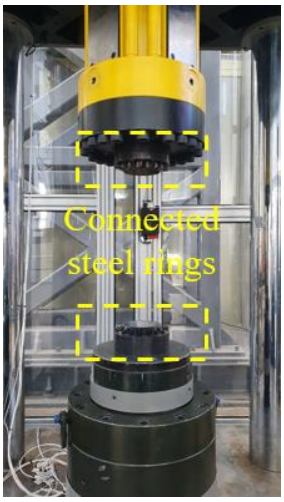

Figure 2.12 Pre-test in the dynamic uniaxial tensile test with only steel rings

The effective mass of the bottom grip is estimated as the average value over time. To accurately evaluate the inertial force of the specimen, the effective mass of the bottom grip for each target pull-out velocity should be determined in advance, thereby calculating the tensile loading applied to the specimen in the dynamic uniaxial tensile test using the high-speed hydraulic machine. Like the static test, dynamic direct tensile stress can be calculated as shown in Eq. 2.10 by dividing the applied loading by the cross-sectional area of the specimen.

$$\sigma_{d,dynamic} = \frac{P}{A_s} \tag{2.10}$$

The average strain rate can be obtained from the time to reach the maximum value of the tensile stress and Young's modulus of the specimen without significant dependence on the strain rate. Eq. 2.11 presents the average strain rate of the specimen in the dynamic uniaxial tensile test using high-speed hydraulic machine.

$$\dot{\varepsilon} = \frac{f_{dd}}{E_s T} \tag{2.11}$$

2.2.3. Requirements for dynamic uniaxial tensile test method

2.2.3.1 Condition of the notch

In the static and dynamic uniaxial tensile tests, it is important to determine test specimen geometry to obtain the direct tensile strength by the pure uniaxial tensile loading. For this purpose, it is advantageous for the tensile failure to occur near the middle section of the specimen. To achieve this objective, the researchers have designed dog-bone shape or dumbbell shape specimens. When using a cylindrical specimen, same as the splitting tensile test specimen, a notch may be applied to the specimen to ensure that the crack initiate at the desired part of the specimen. Li and Ansari (2000) applied 1 in. deep notches to the cylindrical specimen of 4 in. diameters. The notches were cut with a diamond blade saw as shown in Figure 2.13.

Meanwhile, Li and Ansari (2000) glued the specimen to end-caps (grips) with epoxy, and the specimen was connected to spherically seated upper and lower joints through a flexible chain to ensure concentricity as shown in Figure 2.14.

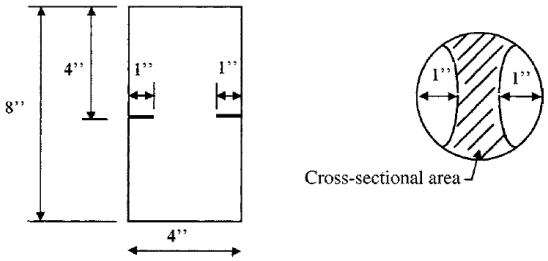

Figure 2.13 Notched specimen using the diamond blade saw (Li and Ansari 2000)

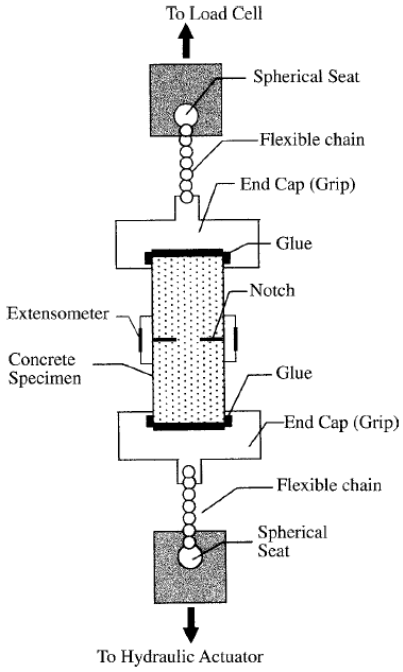

Figure 2.14 Schematics of test setup (Li and Ansari 2000)

Although it is most ideal to obtain valid dynamic direct tensile strength without applying a notch, if the notch is not applied, there is a high probability that the tensile failure occurs around the steel rings rather than

near the middle section of the specimen under uniaxial tensile stress. Applying a notch to the specimen can ensure not only the desired tensile failure behavior but also prevent premature failure of the specimen due to the stress concentration. Therefore, to propose a test method for the dynamic uniaxial tensile test using high-speed hydraulic machine, it is a prerequisite to determine the condition of the notch.

2.2.3.2 Amount of the notch

As previously described, notching the specimen ensures that the crack initiate near the applied notch. When the loading is applied to the notched specimen, the direct tensile strength can be obtained in the uniaxial stress state near the notch. However, a large amount of the notch can cause excessive stress disturbance. If the excessive stress disturbance occurs near the applied notch, obtained direct tensile strength values cannot be regarded as valid values. Hence, an appropriate amount of the notch should be determined to propose a test method for the dynamic uniaxial tensile test using high-speed hydraulic machine.

3. Experimental Program

This chapter covered the details of the preliminary tests to propose dynamic splitting and uniaxial tensile test methods and the main test to suggest splitting and direct tensile DIFs of concrete. First of all, to determine several requirements for each dynamic tensile test method as mentioned in chapter 2, the details of the preliminary tests including test conditions, data post-processing and test results were described. In the following concluding remarks, the dynamic splitting and uniaxial tensile test methods were proposed based on each preliminary test result.

Then, based on the proposed test method, performed main test was explained: test program, data post-processing and test results followed. Finally, after validation of test data, reliable splitting and direct tensile DIFs of concrete were presented.

3.1. Preliminary splitting tensile test

3.1.1. 1st preliminary test

3.1.1.1 Test conditions

Preliminary splitting tensile test was performed twice, and the objective of 1st preliminary test was to determine the specimen dimension. To figure out the change in the experimental strain rate region and the dynamic stress equilibrium according to the specimen dimension, the diameter and Length/Diameter ratio (L/D ratio) of the specimen were considered as test variables. Tables 3.1 presents test variables of 1st preliminary test. Considering

the SHPB bar diameter of 76.2 mm, the diameters of the specimens were selected as 75 and 50 mm, and the L/D ratio was chosen to be 1.0 and 0.5 for the convenience of classification. The length of the striker was selected as a long length of 600 mm to ensure sufficient loading duration of the incident wave. In addition, a 52×48×4 annular pulse shaper made of C1020 copper was used to minimize wave dispersion and to obtain gradually increasing incident waves to satisfy the dynamic stress equilibrium of the specimen.

Dynamic test was conducted twice per one loading condition for a total of 8 specimens. In the static test, the average value of the static splitting tensile strength was obtained by performing the test with the specimen of the same dimension as the dynamic test. Figure 3.1 illustrates the designation of the specimen group considering test variables.

Test specimens were cast in D75×L150 and D50×L100 molds according to ASTM C192/C192M and cured in water using water tank storage following ASTM C511. After curing, the middle part of the specimen was cut using a diamond blade saw to make D75×L75, D75×L38, D50×L50, D50×L25 specimens. Meanwhile, the static compressive strength test was performed on four D150×L300 standard test specimens according to ASTM C39/C39M. As a result, the average static compressive strength and Young's modulus were 38.4 MPa and 24,772 MPa, respectively.

Table 3.1 Test variables of 1st preliminary test (Splitting tensile)

Test variables		Test condition			
Diameter, mm	L/D ratio	Specimen mounting method	Striker length, mm	Impact velocity, m/s	Pulse shaper, mm
50, 75	0.5, 1	Flat loading platen	600	10	52×48×4

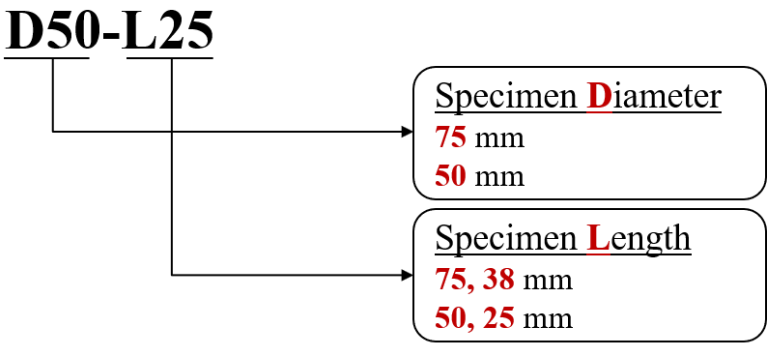

Figure 3.1 Designation of 1st preliminary test specimen group (Splitting tensile)

Figure 3.2 Test specimen of 1st preliminary test (Splitting tensile)

Dynamic splitting tensile test was carried out using 76.2 mm SHPB apparatus of Extreme Performance Testing Center in Seoul National

University as shown in Figure 3.3. And Universal Testing Machine (UTM) of MTS 815 in Seoul National University was used for the static splitting tensile test.

Figure 3.3 SHPB apparatus of EPTC in SNU

Figure 3.4 MTS 815 with the aligning jig in SNU

3.1.1.2 Data post-processing and test results

Using the strain gauges, all strain waves were measured with a sampling rate of 1 MHz. Raw strain waves measured by attached strain gauges were filtered by using a low-pass filter. In other words, frequency spectrums on the incident and transmitted bars exceeding 30 kHz were small enough to be neglected. Therefore, the cut-off frequency of 30 kHz was selected to filter the noise of the raw strain waves.

Tensile DIF of concrete by splitting tensile strength can be expressed as Eq. 3.1. At this moment, tensile DIF at the quasi-static strain rate was considered to be 1.0.

$$DIF_{sp} = \frac{\text{Dynamic splitting tensile strength}}{\text{Static splitting tensile strength}} \tag{3.1}$$

Meanwhile, the dynamic stress equilibrium is a prerequisite in the dynamic splitting tensile test using SHPB. To quantitatively evaluate the dynamic stress equilibrium of the specimen, *R* value suggested by Flores-Johnson and Li (2017) was used. The *R* value indicates the stress difference between the front and back end surfaces of the specimen as shown in Eq. 3.2. As the *R* value is greater, the dynamic stress equilibrium of the specimen deteriorates. Figure 3.5 shows representative dynamic splitting tensile stress-time relationship that have two different *R* values: 3 and 36%.

$$R = \left| \frac{f_{spd,\,front} - f_{spd,\,back}}{f_{spd}} \right| \tag{3.2}$$

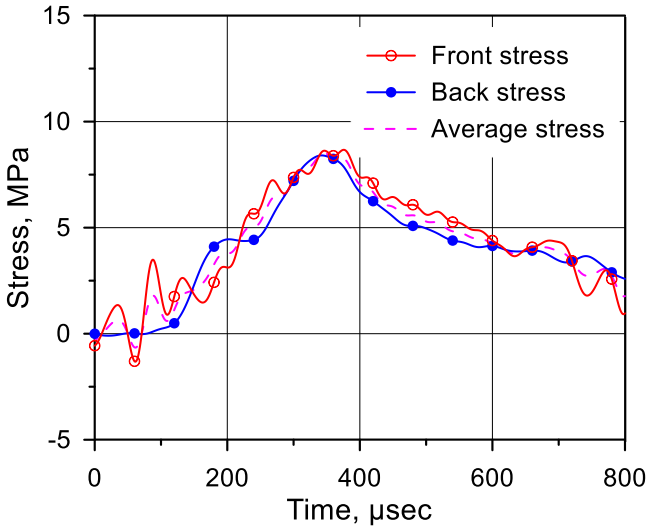

(a)

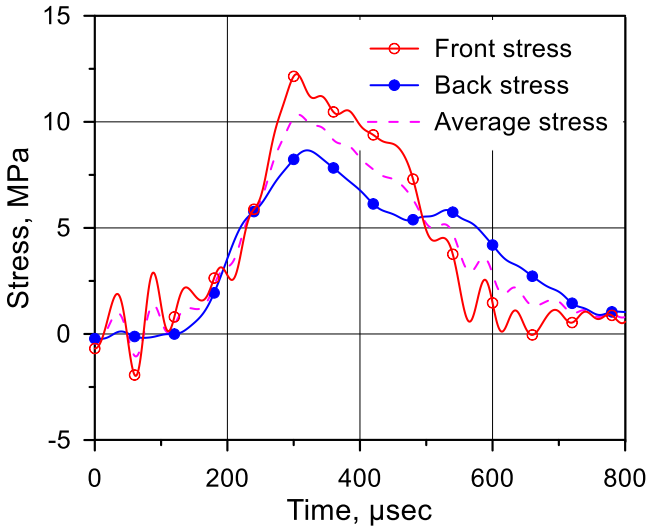

(b)

Figure 3.5 Dynamic splitting tensile stress-time relationship with different *R* values; (a) 3%; (b) 36%

Figure 3.6 shows tensile DIF values versus the common logarithm of the strain rate. Tensile DIF tended to increase as the diameter and the L/D ratio of the specimen increased. However, the increase in the strain rate region according to the specimen dimension was not significant (1-2 s^{-1}). That is, it can be seen that there is a limitation to obtaining an increased experimental strain rate region through a change in the specimen dimension.

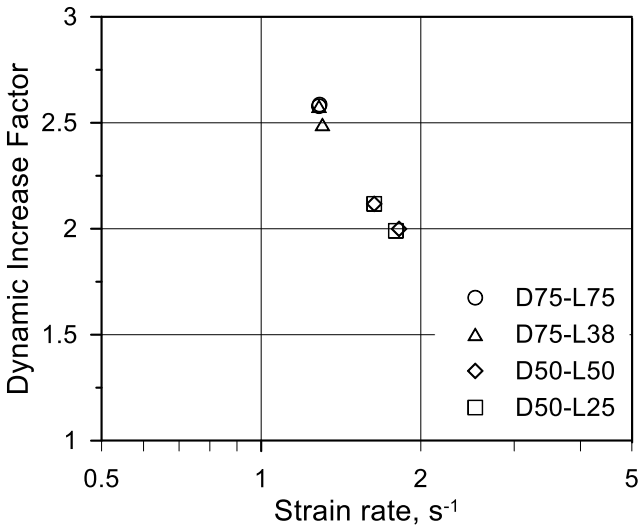

Figure 3.6 Tensile DIF of 1st preliminary test (Splitting tensile)

Figure 3.7 and 3.8 show the *R* values according to test variables: the diameter and the L/D ratio of the specimen. Additionally, Table 3.2 presents the static splitting tensile test results. When the L/D ratio is the same, it can be seen that dynamic stress equilibrium deteriorates as the diameter decreases. And, when the diameter is the same, the small L/D ratio deteriorates the dynamic stress equilibrium of the specimen. In other words, the dynamic stress equilibrium deteriorates as the specimen dimension decreases.

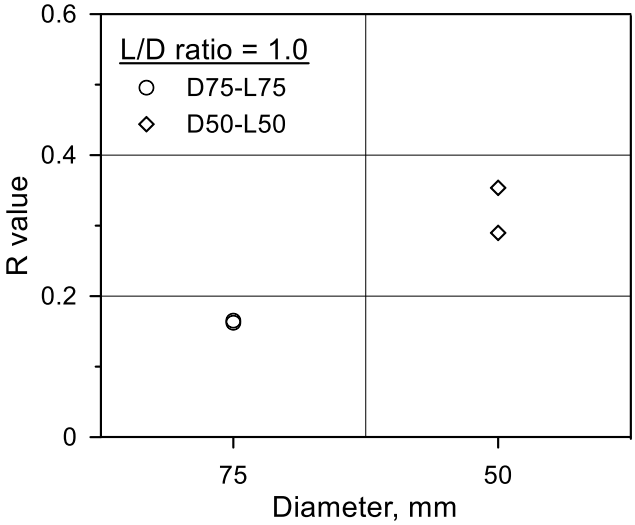

(a)

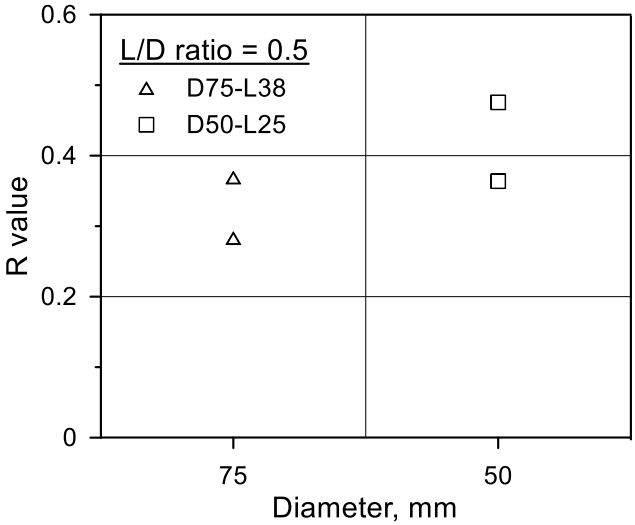

(b)

Figure 3.7 *R* values according to the specimen dimension of 1st preliminary test (Splitting tensile); (a) L/D ratio 1.0; (b) L/D ratio 0.5

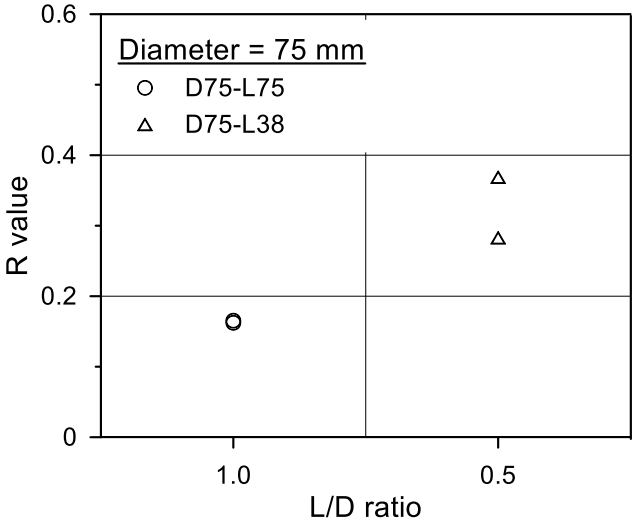

(a)

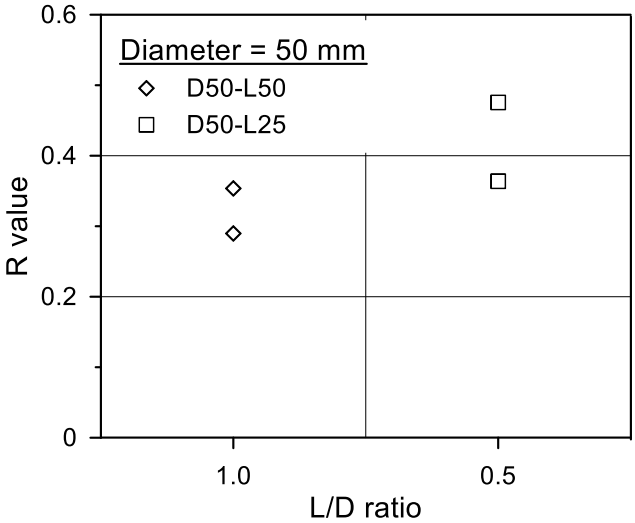

(b)

Figure 3.8 *R* values according to the specimen dimension of 1st preliminary test (Splitting tensile); (a) D75; (b) D50

Table 3.2 Static tensile test results of 1st preliminary test (Splitting tensile)

I.D.	$f_{sp,\ static}$, MPa	I.D.	$f_{sp,\ static}$, MPa
D75-L75	3.79	D50-L50	5.14
D75-L38	3.97	D50-L25	5.16

3.1.1.3 Concluding remarks

From the test results of 1st preliminary test, it was confirmed that the specimen dimension has no significant effect on the change in the strain rate. Furthermore, the smaller the specimen dimension, the worse the dynamic stress equilibrium. Therefore, in consideration of the dynamic stress equilibrium, D75 × L75 was determined to be an appropriate specimen dimension in the dynamic splitting tensile test.

3.1.2. 2nd preliminary test

3.1.2.1 Test conditions

The objective of 2nd preliminary test was to determine the specimen mounting method. Among the main specimen mounting methods, load-bearing strips and arc loading methods have some problems. When the strain waves arrive at the strips or loading plate, the strain waves are reflected and transmitted. Hence, it is difficult to predict the exact strain waves applied to the specimen. In addition, it is not easy to fix the strips or loading plate between the specimen and the bar during the test. In particular, in the case of arc loading, there is a limitation in that it is hard to completely match the radius of the specimen and the radius of curvature of the loading plate.

Therefore, flat loading platen and Flattened Brazilian Disc (FBD) methods were chosen to be compared in this study. Meanwhile, FBD method proposed by Wang et al. (2009) is known to prevent local stress concentration and minimize premature failure due to the concentrated loading by flattening the contact surface of the specimen in contact with the bars. Each specimen mounting method was compared and analyzed according to the strain rate to figure out the appropriate specimen mounting method in the dynamic splitting tensile test. Table 3.3 presents test variables of 2nd preliminary test.

A total of 28 specimens were tested with four specimens per one loading condition including the dynamic and static tests. The average static splitting tensile strength was obtained for each specimen mounting method. Specimen group considering test variables is illustrated in Figure 3.9.

All test specimens were cast using D75×L150 and the designed steel molds for FBD D75 specimens which were fabricated to have a loading angle of 20 degrees as shown in Figure 3.10 and Figure 3.11. Following ASTM C511, test specimens were cured in water using water tank storage, and D75×L75 specimens were made by a diamond blade saw after 28-day curing. Static compressive strength and Young's modulus, which are the static material properties used for test result analysis, were 51.1 MPa and 33,986 MPa, respectively.

Table 3.3 Test variables of 2nd preliminary test (Splitting tensile)

Test variables		Test conditions		
Specimen mounting method	Impact velocity, m/s	Specimen dimension, mm	Striker length, mm	Pulse shaper
Flat loading platen, FBD	8, 10, 12	D75×L75	600	52×48×4

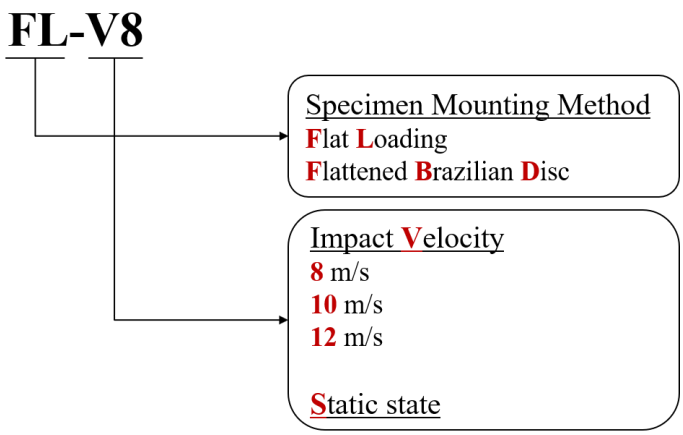

Figure 3.9 Designation of 2nd preliminary test specimen group (Splitting tensile)

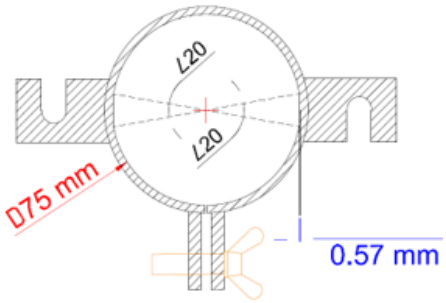

(a)

(b)

Figure 3.10 Designed FBD D75 steel mold; (a) Drawing detail (b) Actual mold

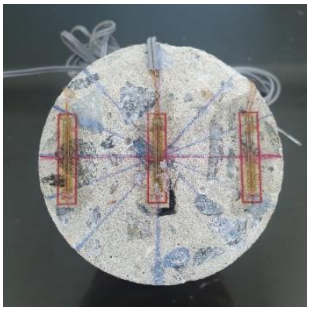

(a)

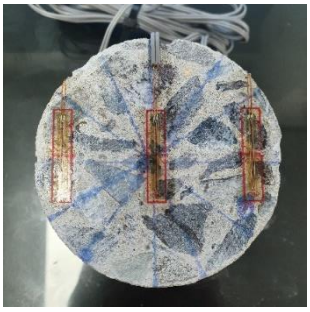

(b)

Figure 3.11 Test specimen of 2nd preliminary test (Splitting tensile); (a) Flat loading platen (b) FBD

3.1.2.2 Data post-processing and test results

Wang et al. (2009) presented a formula for calculating splitting tensile stress of the specimen having a loading angle of 20 degrees as shown in Eq. 3.3. In this study, the splitting tensile strength of FBD specimen was obtained using the same formula in both static and dynamic tests.

$$\sigma_{sp,FBD} = 0.9644 \cdot \frac{2P}{\pi d_s l_s} \tag{3.3}$$

To analyze the test results according to the specimen mounting method, the following three aspects were compared for each specimen mounting method.

1. Tensile DIF and variance of obtained data

2. Evaluation of dynamic stress equilibrium

3. Crack initiation point

First, tensile DIF was calculated using the dynamic splitting tensile strength and static splitting tensile strength for each specimen mounting method. Static splitting tensile strength was 4.11 MPa for flat loading platen and 4.18 MPa for FBD, and Figure 3.12 shows tensile DIF along with the strain rate of 2nd preliminary test.

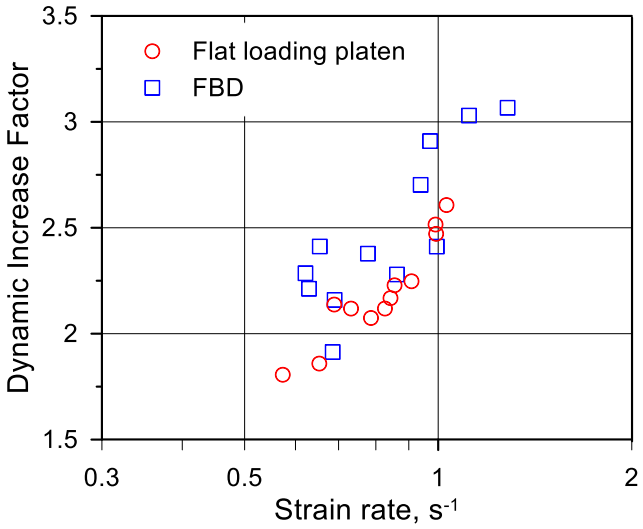

Figure 3.12 Tensile DIF of 2nd preliminary test (Splitting tensile)

As shown in Figure 3.12, it was confirmed that the variance of FBD method data was greater than that of flat loading platen method. Moreover, the second aspect, to evaluate dynamic stress equilibrium, the *R* value for each specimen mounting method was shown in Figure 3.13. As the impact velocity increased, invalid data due to non-dynamic stress equilibrium in both specimen mounting methods increased. In other words, there was no advantage of the FBD method in terms of the dynamic stress equilibrium.

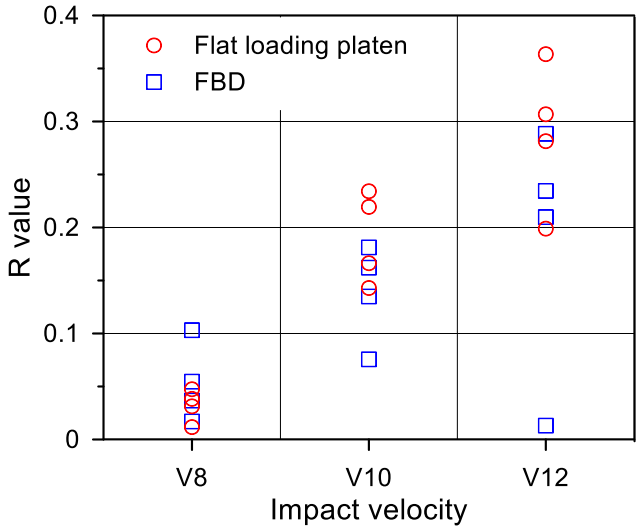

Figure 3.13 *R* values of 2nd preliminary test (Splitting tensile)

Finally, the crack initiation point of the specimen was compared by the specimen mounting method. High-speed camera captured images at 75,000 fps and 512×456 pixels resolution. Figure 3.14 (a) shows the overall failure pattern of flat loading platen method over time when the impact velocity is 10 m/s, and Figure 3.14 (b) shows the dynamic splitting tensile stress at each image point of the same specimen. And the test results of FBD method at the same impact velocity are shown in Figure 3.15. In the case of flat loading platen method, the crack initiation point was observed near the center of all test specimens, whereas in one case of FBD method, the crack initiation point was observed near the contact surface between the specimen and the bar. In other words, FBD method didn't guarantee the center crack initiation.

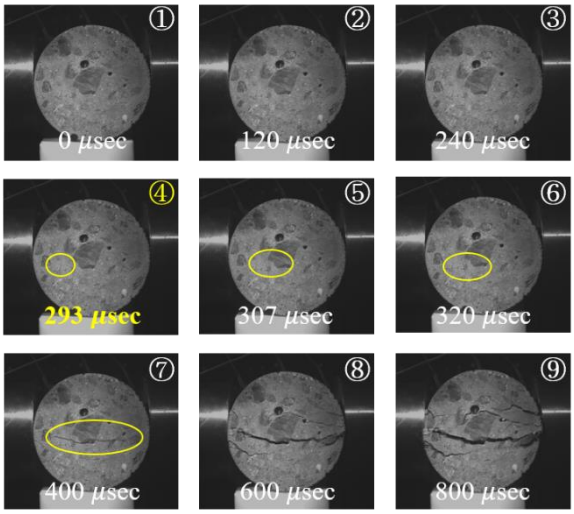

(a)

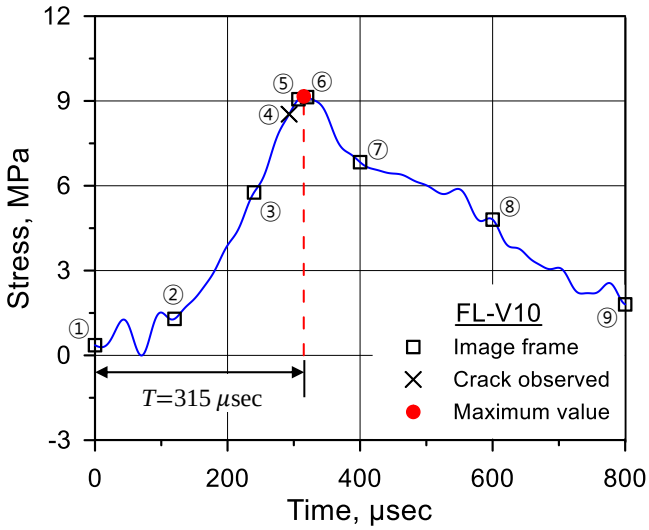

(b)

Figure 3.14 Crack initiation points of 2nd preliminary test (Splitting tensile, impact velocity: 10 m/s, flat loading platen method); (a) Overall failure pattern; (b) Dynamic splitting tensile stress at each image point

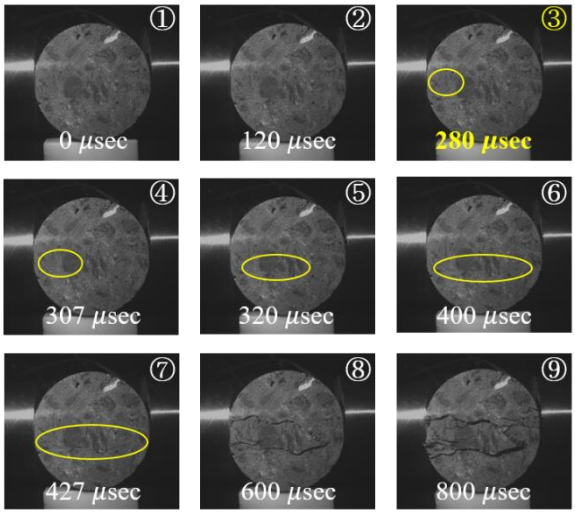

(a)

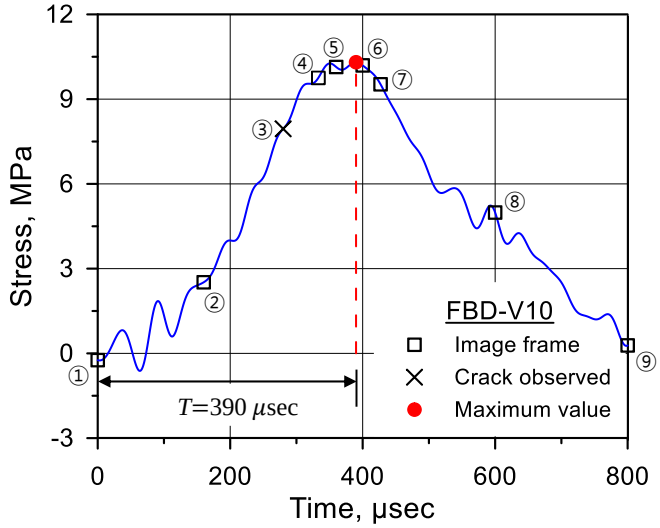

(b)

Figure 3.15 Crack initiation points of 2nd preliminary test (Splitting tensile, impact velocity: 10 m/s, FBD method); (a) Overall failure pattern; (b) Dynamic splitting tensile stress at each image point

3.1.2.3 Concluding remarks

Through 2nd preliminary test, the following contents were confirmed for specimen mounting methods of flat loading platen and FBD methods. FBD method didn't show any distinct advantages over flat loading platen method in terms of data variance, the dynamic stress equilibrium, and the center crack initiation. Therefore, flat loading platen method which needs no additional device was determined to be the appropriate specimen mounting method in the dynamic splitting tensile test.

3.2. Preliminary uniaxial tensile test

3.2.1. 1st preliminary test

3.2.1.1 Test conditions

To propose a test method for the dynamic uniaxial tensile test, it is necessary to determine the condition and amount of the notch. For this purpose, one static preliminary test and one dynamic preliminary test were performed sequentially. The objective of 1st preliminary test was to compare the tensile failure behavior of the specimens according to the condition and amount of the notch in the static test. Table 3.4 presents test variables of 1st preliminary test. Tests were performed with one specimen for each loading condition, and the specimen group considering test variables are illustrated in Figure 3.16.

The diameter of the specimen was to be D75 determined in the splitting tensile test, and the amount of notch was set to D/8 and D/4. The notches were

applied near the middle part of the longitudinal direction of the specimen using a diamond blade saw, and the effective cross-sectional area ratio according to the amount of the notch is shown in Figure 3.17.

Table 3.4 Test variables of 1st preliminary test (Uniaxial tensile)

Test variables		Test conditions
Condition of notch	Amount of notch	Specimen dimension, mm
Un-notched, notched	D/8, D/4	D75×L150

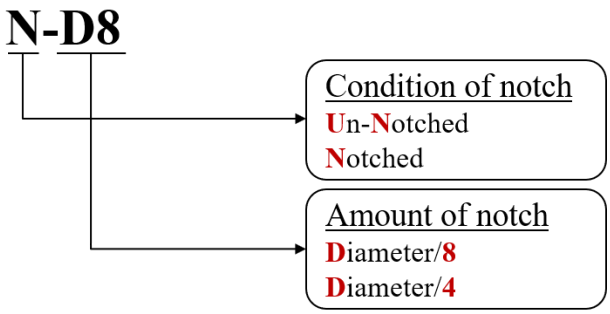

Figure 3.16 Designation of 1st preliminary test specimen group (Uniaxial tensile)

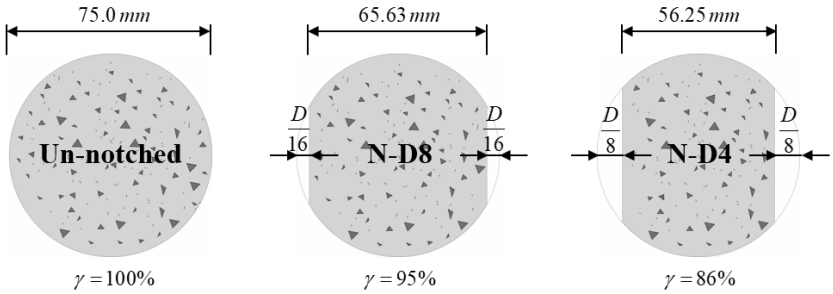

Figure 3.17 Effective cross-sectional area ratio of 1st preliminary test (Uniaxial tensile)

Then, the upper and lower surfaces of the specimen were glued to the steel rings using epoxy. The commercial epoxy of 3M Scotch-Weld 2016 has 22MPa of bonded shear strength at 24℃, and should have enough curing time to get bond capacity. The steel ring and test specimens were aligned through a linear fixture, and the epoxy was cured at 66℃ for 2 hours using an electrical oven. The overall epoxy curing process is shown in Figure 3.18, and test specimen in the uniaxial tensile test is shown in Figure 3.19. Universal Testing Machine (UTM) of MTS 810 in Seoul National University was used for the static uniaxial tensile test.

① Applying epoxy adhesive

② Squeezing (linear fixture) ③ Curing (Oven)

Figure 3.18 Overall epoxy curing process

Figure 3.19 Test specimen of 1st preliminary test (Uniaxial tensile)

Figure 3.20 MTS 810 with the linkage system in SNU

3.2.1.2 Data post-processing and test results

In 1st preliminary test, only the tensile failure behavior of the specimen according to test variables was compared. Tests were performed according to the loading rate targeted at a quasi-static strain rate of 10^{-6} s^{-1}, and the before and after tensile failure are shown in Figure 3.21. As shown in Figure 3.21, in the UN and N-D8 specimens, the tensile failure occurred near the contact between the specimen and the steel ring, whereas the N-D4 specimen showed the tensile failure near the notch.

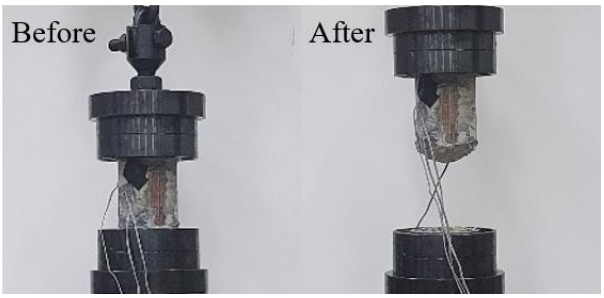

(a)

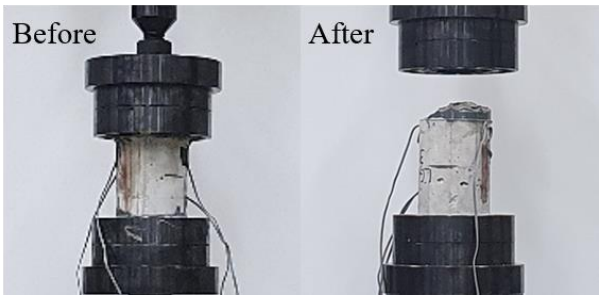

(b)

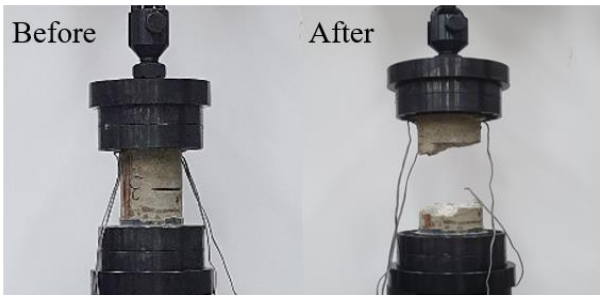

(c)

Figure 3.21 Tensile failure behavior of 1st preliminary test (Uniaxial tensile); (a) UN; (b) N-D8; (c) N-D4

3.2.1.3 Concluding remarks

1st preliminary test results showed that the specimen without a notch could not obtain the desired tensile failure behavior and that a notch of D/4 or higher could ensure the desired tensile failure behavior in the static test. Therefore, in consideration of the tensile failure behavior, more than a D/4 notch is necessary for the uniaxial tensile test.

3.2.2. 2nd preliminary test

3.2.2.1 Test conditions

The objective of 2nd preliminary test was to determine whether the D/4 notch determined in the static test was sufficient in the dynamic test. Test variables of 2nd preliminary test are presented in Table 3.5. Tests were performed with two specimens for each loading condition, and the specimen groups are illustrated in Figure 3.22. The amount of notch was set to be D/4 and D/2, and the effective cross-sectional area ratio according to applied notch

by the diamond blade saw is shown in Figure 3.23. In the same process as 1st preliminary test, the steel rings were bonded to the specimen with epoxy. High-speed hydraulic machine of EPTC in SNU was used for the dynamic test as shown in Figure 3.24. Meanwhile, the pull-out velocity was 10 m/s which is the maximum capacity of high-speed hydraulic machine.

Table 3.5 Test variables of 2nd preliminary test (Uniaxial tensile)

Test variables	Test conditions	
Amount of notch	Specimen dimension, mm	Pull-out velocity, m/s
D/4, D/2	D75×L150	10

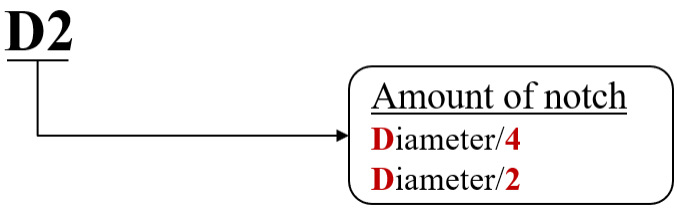

Figure 3.22 Designation of 2nd preliminary test specimen group (Uniaxial tensile)

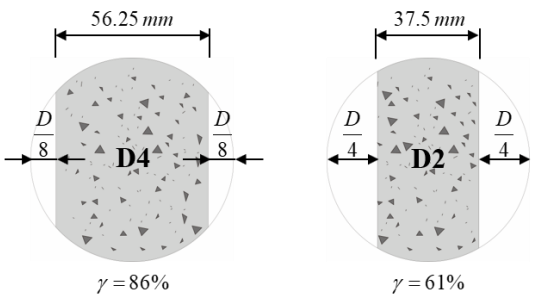

Figure 3.23 Effective cross-sectional area ratio of 2nd preliminary test (Uniaxial tensile)

Figure 3.24 High-speed hydraulic machine of EPTC in SNU

3.2.2.2 Data post-processing and test results

Same as in 1st preliminary test, only the tensile failure behavior of the specimen according to test variables was compared. In the dynamic test, the sampling rate of test data was 1 MHz, and a high-speed camera was used to capture the crack occurrence in the specimen: 40,000 fps and 512×816 pixels resolution. Figure 3.25 (a) and (b) shows the before and the after tensile failure of the D4 specimen and D2 specimen, respectively. As a result, unlike the D/4 notch, the D/2 notch guaranteed the desired tensile failure, which was verified with the high-speed camera images.

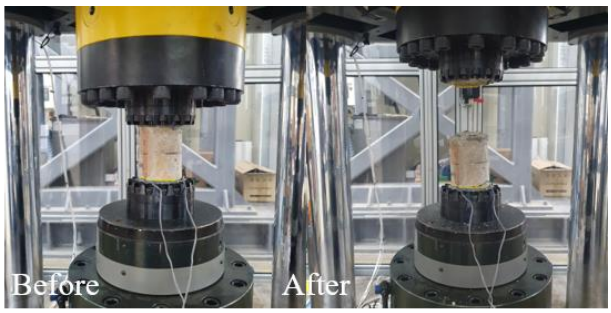

(a)

(b)

Figure 3.25 Tensile failure behavior of 2nd preliminary test (Uniaxial tensile); (a) D4; (b) D2;

3.2.2.3 Concluding remarks

Through 2nd preliminary test to determine the amount of the notch, the specimen having D/2 notch can ensure the desired tensile failure in the dynamic test. Therefore, considering both static and dynamic tests, the amount of the notch was determined to be D/2 for the dynamic uniaxial tensile test method.

3.3. Main test

3.3.1. Test variables

The objective of the main test was to suggest tensile DIF of concrete along with the strain rate. Table 3.6 shows the main test variables that are considered in this study. To evaluate the influence of the static compressive strength on tensile DIF of concrete, three static compressive strengths were considered as test variables. For each type of tensile strength, which is another test variable, the impact and pull-out velocity that simulates transition strain rate region (1-10 s^{-1}) in which the tensile strength rapidly increases was chosen, respectively. Static tensile tests were also conducted with four specimens for each type of strength.

In the main test, a consistent test was carried out by applying the proposed test method through the preliminary test, such as the specimen dimension and specimen mounting method in the dynamic splitting tensile test, and the amount of the notch in the dynamic uniaxial tensile test. Tests were repeatedly performed with four specimens per one loading condition, and Figure 3.26 illustrates the designations of the specimen group for all combinations of the test variables.

Table 3.6 Test variables of the main test

Test variables			Test condition			
			Dynamic splitting tensile test			
f_c', MPa	Type of tensile strength	Impact/ pull-out velocity, m/s	Specimen dimension, mm	Specimen mounting method	Striker length, mm	Pulse shaper
41, 46, 56	Splitting tensile	6, 7, 8, 9	D75×L75	Flat loading platen	600	52×48 ×4
			Dynamic uniaxial tensile test			
	Direct tensile	1, 4, 7, 10	Specimen dimension, mm		Amount of notch	
			D75×L150		D/2	

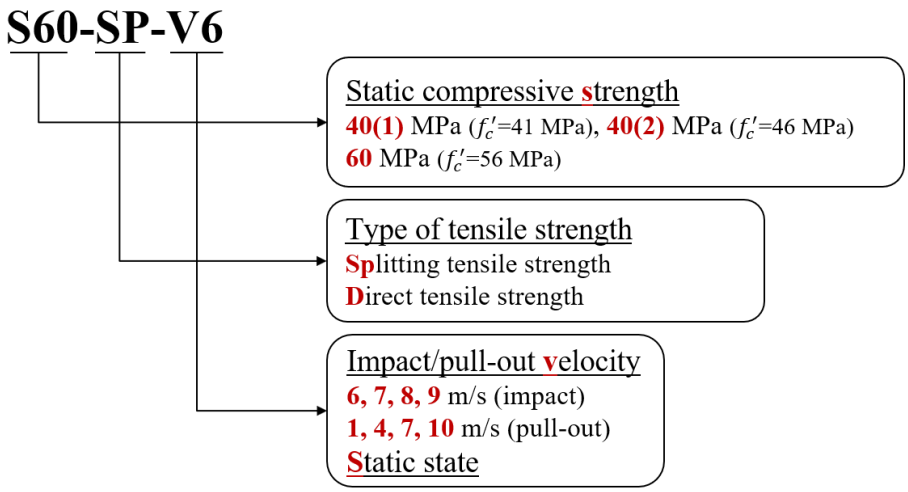

Figure 3.26 Designation of the main test specimen group

3.3.2. Specimen preparation

Table 3.7 shows the concrete mix proportion of the main test. Maximum coarse aggregate size of 25 mm which is commonly used in actual construction sites was used. In the case of the specimens for the static compressive strength tests, concrete was placed in D150×L300 standard cylinder molds. Furthermore, D75×L150 cylinder molds were used for the tensile tests. After 28-day water curing, all test specimens were made in the same way as the preliminary tests. Then, according to ASTM C39/C39M, the averages of the static compressive strength and Young's modulus were obtained as presented in Table 3.8.

Table 3.7 Concrete mix proportion of the main test

f_c', MPa	G_{max}, mm	W/B, %	S/a, %	Unit weight, kg/m^3				
				W	C	S	G	SP*
41		37.0	38.9	170	459	661	1,037	-
46	25	23.1	40.0	111	480	676	1,014	3.1
56		29.4	40.0	141	480	676	1,014	4.2

* Super plasticizer

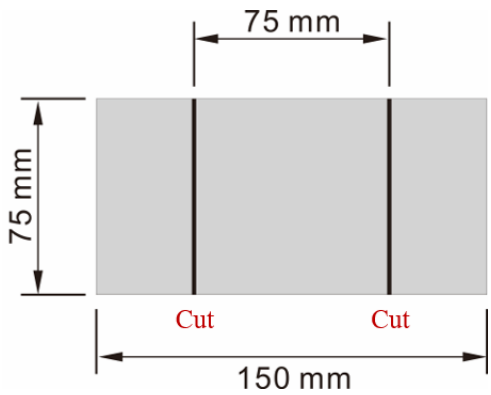

(a)

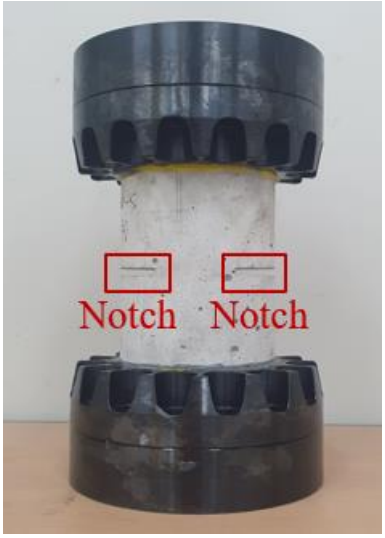

(b)

Figure 3.27 Test specimen of the main test; (a) Splitting tensile test; (b) Uniaxial tensile test

Table 3.8 Static compressive strength test results of the main test

f_c', MPa	Density, kg/m^3	Young's modulus
41.1	2,426	27,338
46.3	2,463	30,199
56.4	2,465	30,726

3.3.3. Data post-processing and test results

Each splitting and uniaxial tensile test was performed in the same test procedure with the same test apparatus as in the preliminary test. In each dynamic test, the sampling rate was 1 MHz, same as the preliminary test, and the loading rate in each static test was determined by targeting the quasi-static strain rate of 10^{-6} s^{-1}. Then, the strain rate was obtained as the average strain

rate. Except for the dynamic direct tensile strength, the tensile strength was defined as the maximum value of the tensile stress. The process of determining the dynamic direct tensile strength is described later.

Meanwhile, splitting tensile DIF of concrete was calculated using Eq. 3.1 previously described. Unlike the preliminary uniaxial tensile test in which only the tensile failure of the specimen was compared, in the main uniaxial tensile test, direct tensile DIF was obtained using Eq. 3.4 below. At this moment, the static and dynamic direct tensile strengths were calculated using Eq 3.5 and Eq. 3.6 by dividing the applied loading by the cross-sectional area of the specimen. To take into account the effective cross-sectional area due to the notch, the effective cross-sectional area ratio according to the D/2 notch of the D75 specimen was used to obtain direct tensile strength.

$$DIF_d = \frac{\text{Dynamic direct tensile strength}}{\text{Static direct tensile strength}} \tag{3.4}$$

$$\sigma_{d,static} = \frac{P}{\gamma A_s} \tag{3.5}$$

$$\sigma_{d,dynamic} = \frac{P}{\gamma A_s} \tag{3.6}$$

Before analyzing the test results, it was necessary to check the validity of the obtained data in the dynamic tests. As previously mentioned, in the dynamic splitting tensile test, the dynamic stress equilibrium was evaluated with the *R* values. In this study, the specimen with the *R* value under or same with 10% was regarded that the dynamic stress equilibrium was satisfied.

Figure 3.28 shows the *R* values of the main splitting tensile test data, and two data exceeding 10% of the *R* value were excluded from the analysis of test results.

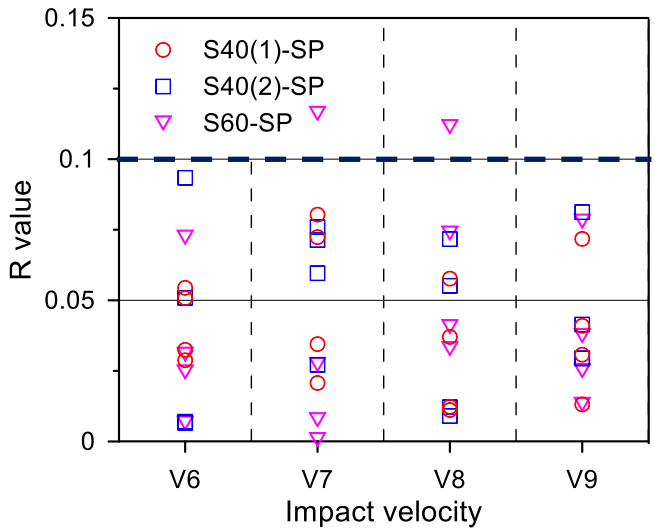

Figure 3.28 *R* values of the main test

As previously described, due to the inertial force of the bottom grip, among several points that can be considered as the tensile strength, the value corresponding to the time at which the crack occurrence is observed through the high-speed camera image was regarded as the tensile strength value. Figure 3.29 (a) and (b) show a representative dynamic direct tensile stress-time relationship and the before and the after of the observed crack occurrence images, respectively.

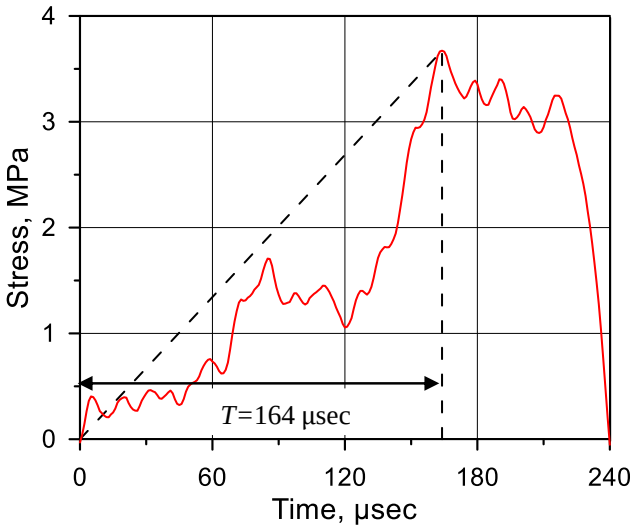

(a)

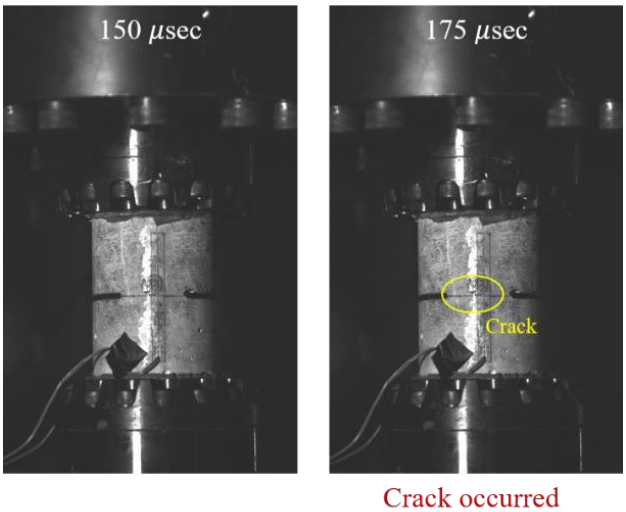

(b)

Figure 3.29 Data-processing of the main test (Uniaxial tensile); (a) Dynamic direct tensile stress-time relationship; (b) Before and the after of the observed crack occurrence images

Meanwhile, there were some problems in conducting the test. If the steel ring and the specimen were not aligned well, the test itself could not be performed because the test machine could not be combined. In addition, when microcracks occurred during specimen fixing or the loading conditions were unstable, very low tensile strength values were obtained. Therefore, these cases were excluded from the analysis of test results as shown in Figure 3.30.

Figure 3.31 shows the relationships between the tensile DIF of concrete and the common logarithm of the strain rate, which are the valid test data of this study. And, Table 3.9 indicates the average values of static tensile strengths used to obtain each tensile DIF in this study.

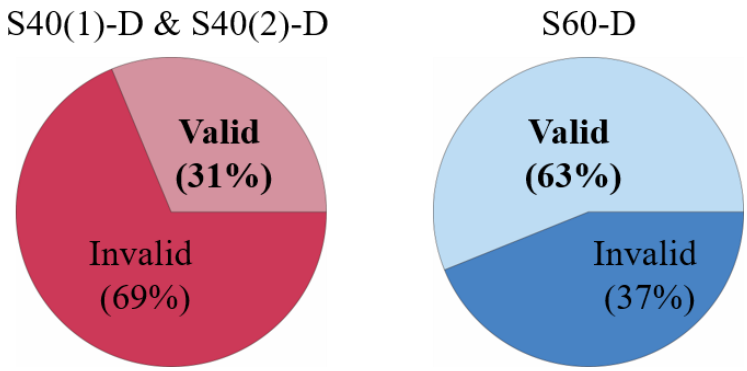

Figure 3.30 Validation of obtained test data in the main test

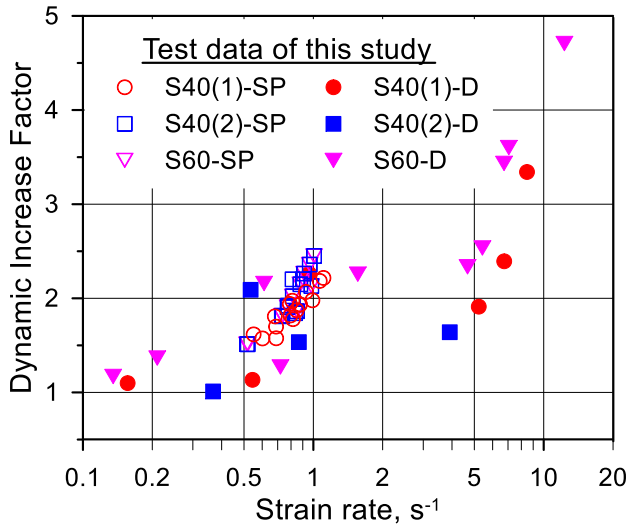

Figure 3.31 Tensile DIF of the main test

Table 3.9 Static tensile test results of the main test

I.D.	$f_{sp,\ static}$, MPa	I.D.	$f_{d,\ static}$, MPa
S40(1)-SP-S	4.19	S40(1)-D-S	2.77
S40(2)-SP-S	4.21	S40(2)-D-S	2.81
S60-SP-S	4.68	S60-D-S	2.89

4. Tensile DIF of Concrete

In this chapter, tensile DIF model of concrete was suggested by nonlinear regression analysis with the obtained test data in chapter 3.3. At this moment, it was discussed in terms of the static compressive strength and the type of tensile strength. In addition, tensile DIF ratio along with the strain rate between splitting and direct tensile DIFs was derived to investigate the relationship between each tensile DIF of concrete.

4.1 Suggestion of tensile DIF model of concrete

First of all, tensile DIF tendency of concrete according to the static compressive strength was examined. Figure 4.1 (a) and (b) present splitting and direct tensile DIFs classified by the type of tensile strength, respectively. Both splitting and direct tensile DIFs showed a similar increase regardless of the static compressive strength. That is, tensile DIF of concrete is not significantly dependent on the static compressive strength.

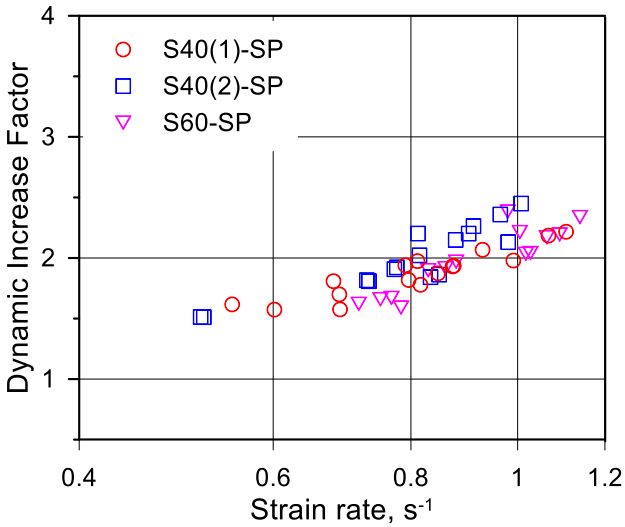

(a)

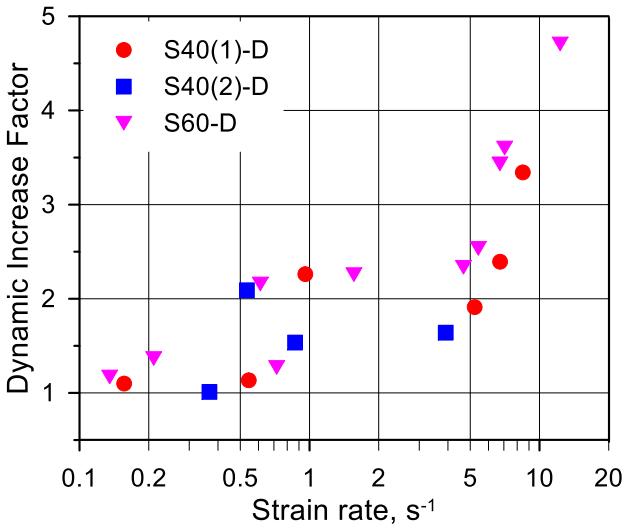

(b)

Figure 4.1 Tensile DIF of concrete according to the static compressive strength; (a) Splitting tensile DIF; (b) Direct tensile DIF

Since the static compressive strength did not have a significant effect on tensile DIF, tensile DIF model considering the type of tensile strength was suggested. Regression analysis was performed concerning the regression model used in the fib MC2010 design code as shown in Eq. 4.1.

$$DIF = k_1 \left(\frac{\dot{\varepsilon}}{\dot{\varepsilon}_s} \right)^{k_2} \tag{4.1}$$

The unknown parameters k_1, k_2 in Eq. 4.1 can be determined by regression analysis based on the obtained test data. At the quasi-static strain rate of the static test, tensile DIF was determined to be 1.0 and a continuous tensile DIF with an inflection point was obtained by diving the strain rate into two sections. Eq. 4.2 presents the regression equation of splitting tensile DIF and Figure 4.2 shows splitting tensile test data and the suggested equation. Then, Eq. 4.3 presents direct tensile DIF regression equation, and uniaxial tensile test data and the suggested equation are shown in Figure 4.3.

$$DIF_{sp} = \begin{cases} \left(\dfrac{\dot{\varepsilon}}{\dot{\varepsilon}_s}\right)^{0.0315} & \text{for } 10^{-6}\,s^{-1} \le \dot{\varepsilon} < 0.54\,s^{-1} \\ 0.000682\left(\dfrac{\dot{\varepsilon}}{\dot{\varepsilon}_s}\right)^{0.583} & \text{for } \dot{\varepsilon} \ge 0.54\,s^{-1} \end{cases} \tag{4.2}$$

where, $\dot{\varepsilon}_s = 1.0 \times 10^{-6}\,s^{-1}$

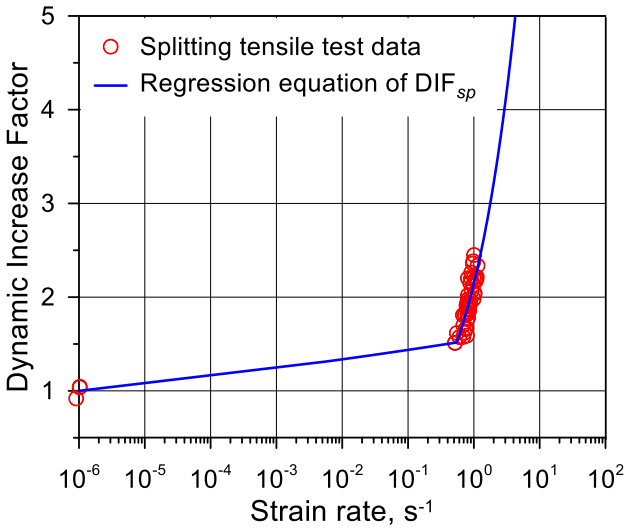

Figure 4.2 Splitting tensile test data and regression equation

$$DIF_d = \begin{cases} \left(\dfrac{\dot{\varepsilon}}{\dot{\varepsilon}_s}\right)^{0.0133} & \text{for } 10^{-6}\,s^{-1} \le \dot{\varepsilon} < 0.21\,s^{-1} \\ 0.04953\left(\dfrac{\dot{\varepsilon}}{\dot{\varepsilon}_s}\right)^{0.259} & \text{for } \dot{\varepsilon} \ge 0.21\,s^{-1} \end{cases} \tag{4.3}$$

where, $\dot{\varepsilon}_s = 1.0 \times 10^{-6}\,s^{-1}$

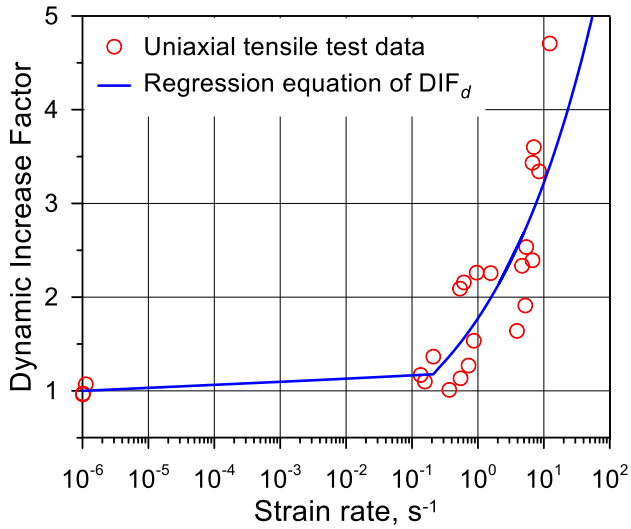

Figure 4.3 Uniaxial tensile test data and regression equation

4.2 Relationship between splitting and direct tensile DIFs

4.2.1. Comparison between splitting and direct tensile DIFs

Figure 4.4 shows the suggested splitting and direct tensile DIF regression equations. Each tensile DIF increases with the strain rate, and shows a rapid increase especially at the inflection point. The disagreement of two tensile DIFs tends to be greater as the strain rate increases. Meanwhile, direct tensile DIF is required in the material model for the numerical analysis of the structures.

However, uniaxial tensile test is complicated in both static and dynamic tests, such as specimen alignment and unexpected crack occurrence, and large variance of test data. Therefore, it is possible to obtain direct tensile DIF with splitting tensile DIF obtained through relatively simple splitting tensile test with low variance of test data. For this purpose, the relationship between splitting and direct tensile DIFs should be investigated.

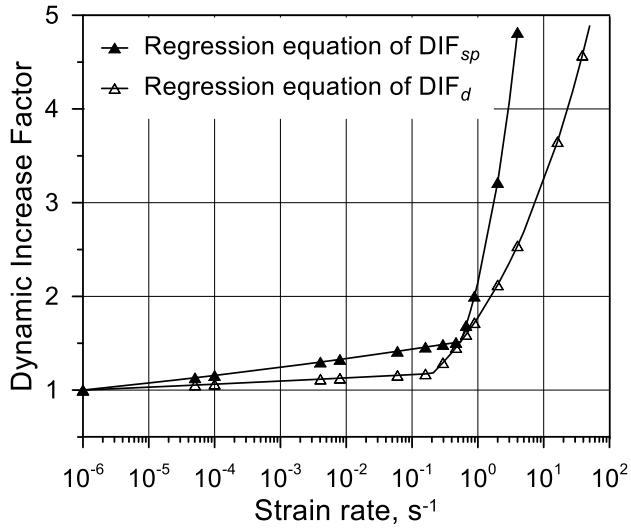

Figure 4.4 Suggested splitting and direct tensile DIF regression equations

4.2.2. Derivation of tensile DIF ratio along with the strain rate

Eq. 4.4 is expressed by dividing the suggested splitting tensile DIF model by direct tensile DIF model. Based on the inflection point of each regression equation, the entire strain rate region was divided into three sections. As shown in Eq. 4.5, direct tensile DIF can be easily obtained by multiplying the derived tensile DIF ratio by splitting tensile DIF in each strain rate section.

$$DIF_{ratio} = \frac{DIF_d}{DIF_{sp}} = \begin{cases} \left(\dfrac{\dot{\varepsilon}}{\dot{\varepsilon}_s}\right)^{-0.0182} & \text{for } 10^{-6}s^{-1} \le \dot{\varepsilon} < 0.21s^{-1} \\ 0.04953\left(\dfrac{\dot{\varepsilon}}{\dot{\varepsilon}_s}\right)^{0.2275} & \text{for } 0.21s^{-1} \le \dot{\varepsilon} < 0.55s^{-1} \\ 72.62\left(\dfrac{\dot{\varepsilon}}{\dot{\varepsilon}_s}\right)^{-0.324} & \text{for } \dot{\varepsilon} \ge 0.55s^{-1} \end{cases} \quad (4.4)$$

$$DIF_{ratio} \times DIF_{sp} = DIF_d \tag{4.5}$$

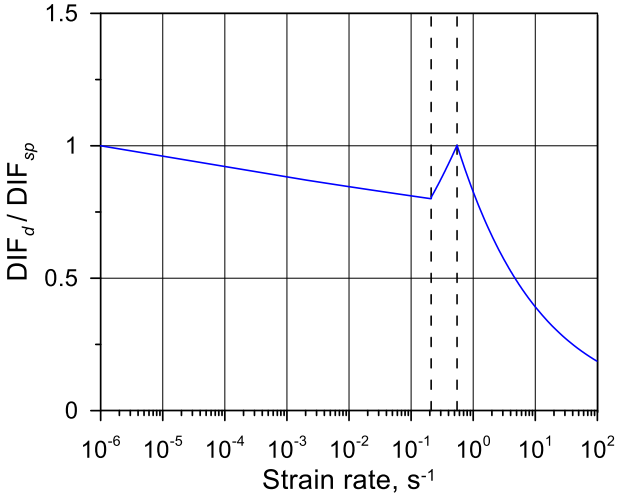

Figure 4.5 Tensile DIF ratio between splitting and direct tensile DIFs

5. Conclusions

Tensile strength enhancement, represented by tensile DIF, is one of the important things for accurate analysis and economical design of concrete structures. Tensile DIF of concrete proposed by many researchers and presented in various design codes has a limitation that it is not obtained through a consistent test due to the absence of a standard test method for the dynamic tensile test. Since the dynamic tests have been conducted through different test methods, different tensile DIFs has been obtained. Therefore, it is necessary to establish a dynamic tensile test method to build a reliable database.

In this study, a series of the preliminary tests were planned and performed to propose the dynamic splitting and uniaxial tensile test methods. In proposing each test method, several requirements to be determined were presented through literature reviews of previous studies and analysis of the static test procedure. In the dynamic splitting tensile test using SHPB, the specimen dimension and specimen mounting method were determined, and in the dynamic uniaxial tensile test using high-speed hydraulic machine, the condition and amount of the notch were determined through the preliminary test results.

By applying proposed test method, reliable tensile DIF data of concrete was obtained for each static compressive strength and the type of tensile strength. Static compressive strength did not have a significant effect on tensile DIF, and through regression analysis, tensile DIF regression equation

as a function of the strain rate was suggested for each type of tensile strength. As the strain rate increases, the difference between splitting and direct tensile DIF was increased.

Meanwhile, in order to obtain direct tensile DIF required for the analysis model using splitting tensile DIF, which can be obtained relatively easily, it was necessary to investigate the relationship between splitting and direct tensile DIFs. For this purpose, tensile DIF ratio along with the strain rate between splitting and direct tensile DIFs was derived.

Consequently, it is recommended to apply dynamic tensile test method proposed in this study when a consistent dynamic test is needed to build a reliable database. Furthermore, tensile DIF ratio can be extended to the material model of actual numerical analysis. Therefore, it is expected that results of this study can be applied to the analysis and design of concrete structures under extreme events.

Reference

ACI Committee 370, “Report for the Design of Concrete Structures for Blast Effects”, Farmington Hills, MI, American Concrete Institute, 2014, pp. 33.

ASTM C39/C39M-20b, “Standard Test Method for Compressive Strength of Cylindrical Concrete Specimens”, West Conshohocken, PA, ASTM International, 2020.

ASTM C192/C192M-19a, “Standard Practice for Making and Curing Concrete Test Specimens in Laboratory”, West Conshohocken, PA, ASTM International, 2019.

ASTM C496/C496M-17, “Standard Test Method for Splitting Tensile Strength of Cylindrical Concrete Specimens”, West Conshohocken, PA, ASTM International, 2017.

ASTM C511, “Standard Specification for Mixing Rooms, Moist Cabinets, Moist Rooms, and Water Storage Tanks Used in the Testing of Hydraulic Cements and Concretes”, West Conshohocken, PA, ASTM International, 2019.

ASTM D2936-20, “Standard Test Method for Direct Tensile Strength of Intact Rock Core Specimens”, West Conshohocken, PA, ASTM International, 2020.

Chen, J., Xiang, D., Wang, Z., Wu, G., and Wang, G., “Dynamic Tensile Strength Enhancement of Concrete in Split Hopkinson Pressure Bar Test”, Advances in Mechanical Engineering, Vol. 10, No. 6, 2018, 1687814018782301.

Chen, W. W., and Song, B., “Split Hopkinson (Kolsky) Bar: design, testing and applications”, Springer Science & Business Media, 2010.

Chen, X., Ge, L., Zhou, J., and Wu, S., “Dynamic Brazilian Test of Concrete using Split Hopkinson Pressure Bar”, Mechanics of Materials, Vol. 41, No. 3., 2009, pp. 252-260.

Chen, X., Wu, S., and Zhou, J., “Quantification of Dynamic Tensile Behavior of Cement-based Materials”, Construction and Building Materials, Vol. 51, 2014, pp. 15-23.

Cusatis, G., “Strain-Rate Effects on Concrete Behavior”, International Journal of Impact Engineering”, Vol. 38, No. 4, 2011, pp. 162-170.

fib Bulletin 65, “Model Code 2010 Final draft Volume 1”, fib Fédération internationale du béton, 2012, pp. 161.

Flores-Johnson, E. A., and Li, Q. M., “Structural Effects on Compressive Strength Enhancement of Concrete-like Materials in a Split Hopkinson Pressure Bar Test”, International Journal of Impact Engineering, Vol. 109, 2017, pp. 408-418.

Gomez, J. T., Shukla, A., and Sharma, A., “Static and Dynamic Behavior of Concrete and Granite in Tension with Damage”, Theoretical and Applied Fracture Mechanics, Vol. 36, No.1, 2001, pp. 37-49.

Jin, X., Hou, C., Fan, X., Lu, C., Yang, H., Shu, X., and Wang, Z., “Quasi-Static and Dynamic Experimental Studies on the Tensile Strength and Failure Pattern of Concrete and Mortar Discs”, Scientific reports, Vol. 7, No. 1, 2017, pp. 1-15.

Kong, X., Fang, Q., Li, Q. M., Wu, H., and Crawford, J. E., “Modified K&C Model for Cratering and Scabbing of Concrete Slabs under Projectile Impact”, International Journal of Impact Engineering, Vol. 108, 2017, pp. 217-228.

Lambert, D. E., and Ross, C. A., “Strain Rate Effects on Dynamic Fracture and Strength”, International Journal of Impact Engineering, Vol. 24, No. 10, 2000, pp. 985-998.

Li, Q., and Ansari, F., “High-Strength Concrete in Uniaxial Tension”, Materials Journal, Vol. 97, No. 1, 2000, pp. 49-57.

Liu, P., Zhou, X., Qian, Q., Berto, F., and Zhou, L., “Dynamic Splitting Tensile Properties of Concrete and Cement Mortar”, Fatigue & Fracture of Engineering Materials & Structures, Vol. 43, No. 4, 2020, pp. 757-770.

Lu, Y. B., and Li, Q. M., “About the Dynamic Uniaxial Tensile Strength of Concrete-like Materials”, International Journal of Impact Engineering, Vol. 38, No. 4, 2011, pp. 162-180.

Malvar, L. J., and Crawford, J. E., “Dynamic Increase Factor for Concrete”, In: 28th Department of Defense Explosives Safety Seminar, Orlando, FL, 1998, pp. 1-17.

Ross, C. A., Tedesco, J. W., and Kuennen, S. T., “Effects on Strain Rate on Concrete Strength”, Materials Journal, Vol. 92, No. 1, 1989, pp. 37-47.

Schuler, H., Mayrhofer, C., and Thoma, K., “Spall Experiments for the Measurement of the Tensile Strength and Fracture Energy of Concrete at High Strain Rates”, International Journal of Impact Engineering, Vol. 32, No. 10, 2006, pp. 1635-1650.

Siregar, R. A., Daimaruya, M., and Fuad, K., “Dynamic Splitting-Tensile Test and Numerical Analysis for Brittle Materials”, AIP Conference Proceedings, American Institute of Physics, Vol. 909, No. 1, 2007, pp. 68-73.

Tedesco, J. W., and Ross, C. A., “Experimental and Numerical Analysis of High Strain Rate Splitting-Tensile Tests”, Materials Journal, Vol. 90, No. 2, 1993, pp. 162-169.

Unified Facilities Criteria (UFC) 3-340-02, “Structures to Resist the Effects of Accidental Explosions”, Washington D.C., U.S. Department of Defense, 2008, pp. 1065-1066.

Wang, Q.Z., Li, W., and Xie, H. P., “Dynamic Split Tensile Test of Flattened Brazilian Disc of Rock with SHPB Setup”, Mechanics of Materials, Vol. 41, No. 3, 2009, pp. 252-260.

Xu, H., and We, H. M., “Semi-Empirical Equations for the Dynamic Strength Enhancement of Concrete-like Materials”, International Journal of Impact Engineering, Vol. 60, 2013, pp. 76-81.

Yang, F., Ma, H., Jing, L., Zhao, L., and Wang, Z., “Dynamic Compressive and Splitting Tensile Tests on Mortar using Split Hopkinson Pressure Bar Technique”, Latin American Journal of Solids and Structures, Vol. 12, No. 4, 2015, pp. 730-746.

Zheng, W., Kwan, A. K. H., and Lee, P. K. K., “Direct Tension Test of Concrete”, Materials Journal, Vol. 98, No. 1, 2001, pp. 63-71.

국문초록

콘크리트의 인장 동적증가계수 획득을 위한 동적 쪼갬과 일축인장 실험 방법

이 겨 레

일반 설계 수명보다 현저히 긴 재현주기를 가지는 극단 상황에 의한 하중은 동적 하중으로 특정 지어진다. 이러한 동적 하중은 구조물에 높은 변형속도를 가하고, 극단 상황 하 구조적 거동은 정적 하중 조건과는 다르다. 따라서, 극단 상황 하 구조물의 정확한 분석과 경제적인 설계를 위해서는 동적 재료 특성을 선행적으로 조사해야 한다.

대표적인 건설자재 중 하나인 콘크리트는 변형률 의존 특성을 지닌 재료이다. 다시 말해 콘크리트의 재료 특성은 변형률 속도에 따라 달라진다. 중요 인자는 압축강도와 인장강도이며, 콘크리트의 각 강도는 변형률 속도가 증가할수록 증가한다. 동적증가계수는 이러한 변형 속도 효과를 기반으로 강도증진을 고려하는 데 사용되며, 정적 재료 특성에 대한 동적 재료 특성의 비로 표현된다.

특히, 인장 동적증가계수로 표현되는 콘크리트의 인장강도증진은 세 가지 이유로 매우 중요하다. 첫째로, 1~100 /s 의 높은 변형률 속도 영역에서 인장강도는 정적 인장강도에 비해 약 2~6 배 증진된다. 비슷한 변형률 속도 구간에서 약 1~2 배 증진되는 압축강도보다 상대적으로 증진비가 높기 때문에, 높은 변형률 속도에서 인장강도는 중요한 고려 사항이다. 둘째로, 동적 인장강도는 폭발과 충돌 하중을 받는 콘크리트와 같은 재료 구조물의 인장파괴를 제어하는데, 구조물의 파편화. 폭열과 배면 파쇄에 지배적인 영향을 미친다. 셋째, 서로 다른 인장 동적증가계수를 사용할 경우 실제 구조물의 수치해석적 시뮬레이션 결과에서 서로 다른 파괴 모드가 발생한다. 이러한 이유로, 동적 하중을 받는 구조적 거동을 이해하기 위해서는 정확한 인장 동적증가계수에 대한 조사가 필요하다.

많은 연구자들이 정적과 동적 인장 실험을 수행하여 콘크리트의 인장 동적증가계수를 제안했으며, 여러 설계 코드에도 다양하게 제시되었다. 하지만, 표준실험 방법이 제시된 정적 인장 실험과 달리 동적 인장 실험에서는 아직 표준실험 방법이 정립되지 않았다. 다양한 연구자들이 다양한 방식으로 동적 인장 실험을 수행했으며, 결과적으로 제안된 인장 동적증가계수가 서로 다르다. 따라서, 일관된 동적 인장 실험을 통해 정확한 인장 동적증가계수를 획득하는 것이 필요하다.

본 연구에서는 일련의 예비 실험을 통해 동적 쪼갬과 일축인장 실험 방법을 제안하였다. 그리고 제안된 실험 방법을 적용하여 콘크리트의 쪼갬과 직접인장 동적증가계수를 획득하기 위한 본 실험을 수행하였다. 변형률 속도에 따른 동적증가계수 곡선을 나타내기 위해 동적증가계수를 1.0 으로 하는 준정적 변형률 속도 값을 획득하기 위한 정적 인장 실험도 수행하였다. 이후 신뢰도 높은 데이터를 바탕으로 회귀분석을 수행하여 쪼갬과 직접인장 동적증가계수 모델을 각각 제안하였다. 제안된 쪼갬과 직접인장 동적증가계수는 변형률 속도가 증가함에 따라 증가하였으며, 두 콘크리트 인장 동적증가계수 모델 간의 관계를 파악하기 위한 인장 동적증가계수 비를 제안하였다.

본 연구에서 제안한 콘크리트의 동적 인장 실험 방법과 인장 동적증가계수 모델은 극단 상황 하 콘크리트 구조물의 분석과 설계에 적용될 수 있을 것으로 기대된다.

주요어: 쪼갬인장 실험, 일축인장 실험, 쪼갬인장강도, 직접인장강도, 인장 동적증가계수, 변형률 속도, 표준실험 방법

학번: 2020-23033